

# **Dye-Surfactant Complex Formation at Low Surfactant Concentration**



Islamabad

**Master of Philosophy**

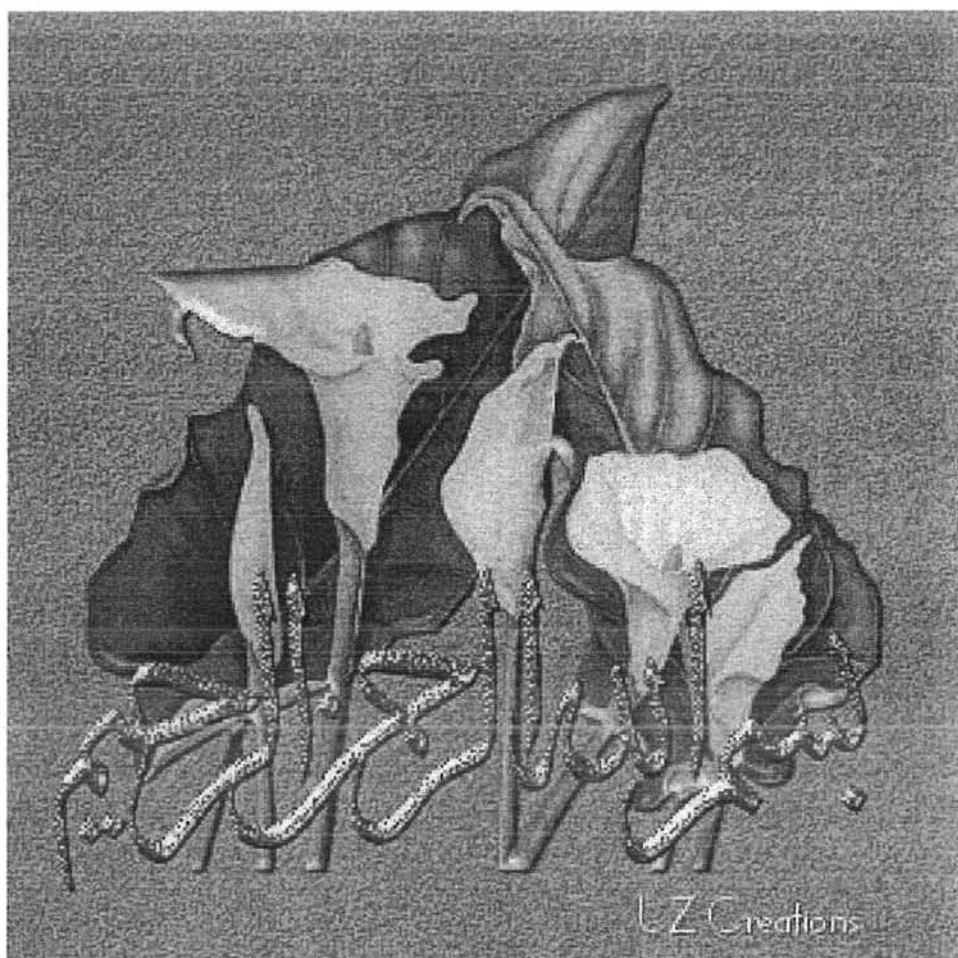
In

**Physical Chemistry**

By

**Fatima Gul**

Department of Chemistry  
Quaid-i-Azam University  
Islamabad  
2008



**IN THE NAME OF ALLAH  
THE COMPASSIONATE  
THE MERCIFUL**

**“Allah will exalt those who believe among you, and  
those have knowledge to high ranks”**

**(Al-Quran)**

**Sayings of Holy Prophet (S.A.W.)**

**“If anybody goes on his way in search of knowledge,  
Allah Almighty will make easy for him the way to  
paradise”**

**(Sahih Muslim)**



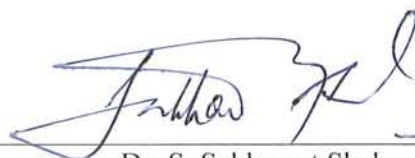
## CERTIFICATE

This is to certify that this dissertation submitted by *Ms. Fatima Gul* is accepted in its present form by the Department of Chemistry, Quaid-i-Azam University, Islamabad, Pakistan, as satisfying the partial requirement for the degree of *Master of Philosophy in Physical Chemistry*.

External Examiner:



Supervisor:



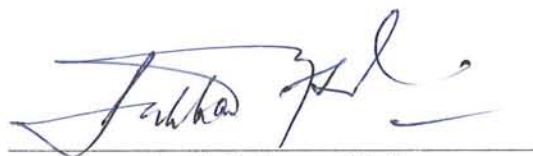
Dr. S. Sakhawat Shah  
Meritorious Professor  
Department of Chemistry  
Quaid-i-Azam University  
Islamabad.

Head of Section:



Prof. Dr. M. Javid Iqbal  
Department of Chemistry  
Quaid-i-Azam University  
Islamabad.

Chairman:



Dr. S. Sakhawat Shah  
Meritorious Professor  
Department of Chemistry  
Quaid-i-Azam University  
Islamabad.

# DEDICATED

To

**My Sweet Baba Jan**

A symbol of success and love for me  
Whose prayers, efforts, financial assistance  
Enable me to reach at this position

**Ammi Jan**

A symbol of affection and kindness  
Whose love and prayers enlightened my path

**Mamu Jan & Bhai Jan**  
(Zakir Khan, Imran Khan & Kamran Khan)

Whose mature and valuable guidance  
Enabled me to perceive & pursue higher aims in life

**My Teacher**  
**Gauhar Sani**

**My Sweet friendly brothers**  
**Shams ul Islam, Saif ul Islam & Dr. Zia ul Islam**

Who are shelter for me who always prove a torch in the darkness  
Of difficulties, Problems & hurdles in the way of my life

**My Cousins**  
**My all family members**  
**My friends**

**Who are the assets of my life**

## ACKNOWLEDGEMENTS

---

All praises to Almighty **Allah**, the creator of creatures of universe and who created us as a Muslim and blessed us with the knowledge to differentiate between right & wrong. Many thanks to Him who bestowed me with sight to observe and mind to think and judge. Peace and blessing of Allah be upon the Holy Prophet, who exhorted his followers to seek for knowledge from cradle to grave. The **Prophet (Swallalaho Alaihe wasallam)** enabled us to worship only one Allah. He (**Sallalaho Alaihe wasallam**) brought out of darkness and enlightened the way of Heaven.

I feel great pleasure in expressing my ineffable thanks to my encouraging, inspirational, cool minded supervisor , **Prof.Dr.Syed Sakhawat Shah** (Prof & chairman Deptt of Chemistry QAU Islamabad) whose personal interest, through provoking guidance, valuable suggestions and discussions enabled me to complete this tedious work, he really encouraged all my attempts to design this research work and provided necessary research facilities.

Heartfelt thanks are to all faculty members, especially to all teachers of Physical section for their morale boosting and encouraging behavior.

Special thanks are due to **Asad Muhammad Khan** whose valuable suggestions enabled me to produce the present work.

I would like to express my sincere thanks and appreciation to my sincere lab fellows **Muhammad Arshad Khosa, Muhammad Faizan, Raheel, Shumaila and Tahira** and friends, **Neelam, Nadia, Farzana, Anisa, Nasreen, Afshan, Jaweria, Gulnaz, Maryam, Sumaira Shah, Iram, Nazia, Naila, Azra, Asma and Nisho.**

Finally I offer my sincere thanks to my family members for their prayers, encouragement and appreciation.

**Fatima Gul**

## Table of Contents

Chapter	Title	Page No
	Acknowledgements	
	Contents	
	Abstract	i
	List of tables	ii-iii
	List of figures	iv-vi
<b>Chapter I</b>		1-3
	Introduction	1
	Aims and Objectives	3
<b>Chapter II</b>		4-48
	Theoretical background	4
	Part I	4
2.1	The Anomalous Properties of Water	4
2.2	Hydrophobic Hydration	5
2.3	Hydrophobic Interactions	6
2.4	Surfactants	6
2.4.1	Surfactants of natural and synthetic origin	8
2.4.2	Structure of Surfactant	9
2.4.3	Classification of Surfactants	9
2.4.4	Properties of Surfactants	13
2.5	Aggregation behavior of surfactants	14
2.5.1	Energy of formation of micelles	15
2.5.2	Critical Micelle Concentration	16
2.5.3	CMC Measurements	17
2.5.4	Factors Affecting CMC in Aqueous Solution	19
2.5.5	Solubilization	19
2.5.6	Locus of Solubilization	20
2.5.7	Factors Affecting Solubilization	20

Chapter	Title	Page No
	Part II	21-29
2.6	Dyes	21
2.6.1	Classification of Dyes	21
2.6.1.1	Classification Of Dyes On The Basis Of mode Of Action	22
2.6.1.2	Food dyes	26
2.6.1.3	Other important dyes	26
2.6.1.4	Natural dyes	27
2.6.1.5	Chemical classification	27
2.6.2	Application of Dyes	27
	Part III	30-34
2.7	Ultraviolet Visible Spectroscopy	30
	Part IV	35-41
2.8	Dye–Surfactant Complex Formation	35
2.8.1	Potentiometry	35
2.8.2	Conductometry	35
2.8.3	Spectroscopic investigation of dye–surfactant ion pair formation in aqueous solution	36
	Part V	42-48
2.9	Literature Review	42
<b>Chapter III</b>		49-51
3.1	Experimental	49
3.1.1	Chemicals	49
3.1.2	Solution Preparation	49
3.1.2.1	Solution preparation for the determination of the composition of the complex	50
3.1.2.2	Solutions for the determination of the equilibrium complex formation constant at 25°C	50
3.1.2.3	Solutions for the determination of the equilibrium complex formation constant at different temperatures	50

Chapter	Title	Page No
3.2	Ultraviolet Visible Spectroscopy	51
3.2.1	Double-Beam Spectrophotometer	51
3.2.2	Measurement of Simple Absorption Spectra	51
<b>Chapter IV</b>	<b>Results and Discussions</b>	<b>52</b>
4.1	Spectrophotometric Study of ARS-CTAB Complex Using Job's Method	52
4.1.1	Equations Used For The Determination Of Different Parameters Of The Complex	53
4.1.2	Calculations Of Thermodynamic Parameters	55
	Section I	56
4.1.3	Part I	56
4.1.3.1	Selection Of The Concentration Range Of The Dye	56
4.1.3.2	Selection Of The Concentration Range Of The Surfactant And wavelength Of the Dye To be Considered	59
4.1.3.3	Determination Of The Composition Of The Complex	63
4.1.3.3.1	Determination Of the Composition Of Complex when $C_S^0 = C_D^0 = 2 \times 10^{-4} \text{ mol.dm}^{-3}$	65
4.1.3.3.2	Determination Of the Composition Of Complex when $C_S^0 = C_D^0 = 1 \times 10^{-4} \text{ mol.dm}^{-3}$	68
4.1.3.4	Determination of equilibrium Complex formation Constant at Room Temperature	71
4.1.3.4.1	Determination Of Equilibrium Complex Formation Constant When $C_S^0 = 3 \times 10^{-4} \text{ mol.dm}^{-3}$ and $C_D^0 = 3 \times 10^{-5} \text{ mol.dm}^{-3}$	72
4.1.3.4.2	Determination Of Equilibrium Complex Formation Constant When $C_S^0 = 3 \times 10^{-4} \text{ mol.dm}^{-3}$ and $C_D^0 = 6 \times 10^{-5} \text{ mol.dm}^{-3}$	75

Chapter	Title	Page No
4.1.3.4.3	Determination Of Equilibrium Complex Formation Constant When $C_S^{\circ}=3 \times 10^{-4} \text{ mol.dm}^{-3}$ and $C_D^{\circ}=8 \times 10^{-5} \text{ mol.dm}^{-3}$	78
4.1.4	PART II	82
4.1.4.1	Determination of $K_{eq}$ at different Temperatures	82
4.1.4.1.1	Determination of $K_{eq}$ at 20 °C	82
4.1.4.1.2	Determination of Equilibrium Complex formation constant at 25 °C	85
4.1.4.1.3	Determination of Equilibrium Complex formation constant at 30 °C	88
4.1.4.1.4	Determination of Equilibrium Complex formation constant at 35 °C	90
4.1.4.1.5	Determination of Equilibrium Complex formation constant at 40 °C	93
4.1.4.2	Thermodynamic Parameters	96
	Section II	99
4.2	Infrared Spectroscopy	99
4.2.1	Applications of Infrared Spectroscopy	100
4.2.1.1	FTIR Study OF ARS-CTAB Complex	101
4.2.1.1.1	FTIR spectrum of CTAB	102
4.2.1.1.2	FTIR spectrum of ARS	104
4.2.1.1.3	FTIR spectrum of ARS-CTAB complex	105
4.3	Suggestion for the possible mechanism of interactions between ARS and CTAB	106
4.4	Conclusions	108
	Future Plans	109
Chapter V	References	110-112

## ABSTRACT

---

Alizarin Red S (ARS), an anthraquinoid dye, forms anionic moiety in aqueous solution. The complex formation of ARS was studied with the cationic surfactant cetyltrimethylammonium bromide (CTAB) in aqueous environment at low surfactant concentrations. The complex was studied with the help of UV-Visible spectroscopy and FTIR technique. Method of continuous variation was applied to check the complex formation. 1:1 complex formation was evident from the experimental results. Equilibrium complex formation constant was determined at room temperature and also at five different temperatures. Different thermodynamic parameters,  $\Delta G$ ,  $\Delta H$  and  $\Delta S$  were also calculated.  $\Delta H$  was calculated using Van't Hoff plot. Structure of the complex was proposed by taking FTIR spectrum of the complex and its correlation with the FTIR spectra of ARS and CTAB.



## INDEX OF TABLES

Table NO	Title	Page No
Table 3.1	Data Including Chemicals with Abbreviations, Molecular Weight and Supplier	49
Table 4.1	Absorbance and maximum wavelength of ARS in aqueous solutions of CTAB	61
Table 4.2	Calculations for the corrected absorbance of the complex formed as a result of interactions between ARS & CTAB ( $C_s^{\circ}=C_D^{\circ}=2 \times 10^{-4} \text{ mol. dm}^{-3}$ )	66
Table 4.3	Calculations for the corrected absorbance of the complex formed as a result of interactions b/w ARS & CTAB ( $C_s^{\circ}=C_D^{\circ}=1 \times 10^{-4} \text{ mol. dm}^{-3}$ )	69
Table 4.4	Calculations for the corrected absorbance of the complex formed as a result of interactions b/w ARS & CTAB ( $C_s^{\circ}= 3 \times 10^{-4} \text{ mol. dm}^{-3}$ , $C_D^{\circ}=3 \times 10^{-5} \text{ mol. dm}^{-3}$ )	73
Table 4.5	Calculations of $K_{eq}$ when $C_s^{\circ}=3 \times 10^{-4} \text{ mol. dm}^{-3}$ and $C_D^{\circ}=3 \times 10^{-5} \text{ mol. dm}^{-3}$	74
Table 4.6	Calculations for the corrected absorbance of the complex formed as a result of interactions b/w ARS & CTAB ( $C_s^{\circ}= 3 \times 10^{-4} \text{ mol. dm}^{-3}$ , $C_D^{\circ}=6 \times 10^{-5} \text{ mol. dm}^{-3}$ )	76
Table 4.7	Calculations of $K_{eq}$ when $C_s^{\circ}=3 \times 10^{-4} \text{ mol. dm}^{-3}$ and $C_D^{\circ}=6 \times 10^{-5} \text{ mol. dm}^{-3}$	77
Table 4.8	Calculations for the corrected absorbance of the complex formed as a result of interactions b/w ARS & CTAB ( $C_s^{\circ}= 3 \times 10^{-4} \text{ mol. dm}^{-3}$ , $C_D^{\circ}=8 \times 10^{-5} \text{ mol. dm}^{-3}$ )	79
Table 4.9	Calculations of $K_{eq}$ when $C_s^{\circ}=3 \times 10^{-4} \text{ mol. dm}^{-3}$ and $C_D^{\circ}=8 \times 10^{-5} \text{ mol. dm}^{-3}$	80
Table 4.10	Calculations for the corrected absorbance of the complex formed as a result of interactions between ARS and CTAB at 20°C	83
Table 4.11	Calculations of $K_{eq}$ at 20°C	84

Table NO	Title	Page No
Table 4.12	Calculations for the corrected absorbance of the complex formed as a result of interactions between ARS and CTAB at 25°C	86
Table 4.13	Calculations of $K_{eq}$ at 25°C	87
Table 4.14	Calculations for the corrected absorbance of the complex formed as a result of interactions between ARS and CTAB at 30°C	89
Table 4.15	Calculations of $K_{eq}$ at 30°C	90
Table 4.16	Calculations for the corrected absorbance of the complex formed as a result of interactions between ARS and CTAB at 35°C	91
Table 4.17	Calculations of $K_{eq}$ at 35°C	92
Table 4.18	Calculations for the corrected absorbance of the complex formed as a result of interactions between ARS and CTAB at 40°C	94
Table 4.19	Calculations of $K_{eq}$ at 40 °C	95
Table 4.20	Values of $K_{eq}$ at different temperatures	96
Table 4.21	Calculations of different thermodynamic parameters	98

## INDEX OF FIGURES

Figure No	Caption	Page No
Figure 2.1	Chemical structure of Sodium dodecylsulphate	10
Figure 2.2	Chemical structure of Cationic surfactant	11
Figure 2.3	Chemical structure of Nonionic surfactant	11
Figure 2.4	Chemical structure of Zwitterionic surfactant	12
Figure 2.5	Different transitions in UV-Visible region	31
Figure 4.1	UV-Visible spectra of Alizarin Red S in aqueous medium	57
Figure 4.2	Plot of absorbance Vs. wavelength of different concentrations of ARS in aqueous medium	58
Figure 4.3	Plot of absorbance Vs. concentration of ARS in aqueous medium	58
Figure 4.4	Visible absorption spectra of ARS ( $5 \times 10^{-5} \text{ mol.dm}^{-3}$ ) at various concentration of Cetyltrimethylammonium bromide (CTAB) at 298K	60
Figure 4.5	Plot of absorbance Vs. concentration of the complex from premicellar to post-micellar concentrations of CTAB	62
Figure 4.6	Plot of $\lambda_{\text{max}}$ Vs. concentration of the complex from premicellar to post-micellar concentrations of CTAB	62
Figure 4.7	Plot of Absorbance Vs. wavelength of different volume fractions of the complex made from equimolar mother solutions of ARS and CTAB ( $C_S^0 = C_D^0 = 2 \times 10^{-4} \text{ mol.dm}^{-3}$ )	65
Figure 4.8	Job's plot for equimolar mother solutions of ARS and CTAB in water at 298K. $C_S^0 = C_D^0 = 2 \times 10^{-4} \text{ mol.dm}^{-3}$	67
Figure 4.9	Plot of Absorbance Vs. wavelength of different volume fractions of the complex made from equimolar mother solutions of ARS and CTAB ( $C_S^0 = C_D^0 = 1 \times 10^{-4} \text{ mol.dm}^{-3}$ )	68

Figure No	Caption	Page No
Figure 4.10	Job's plot for equimolar mother solutions of ARS and CTAB in water at 298K. $C_S^0 = C_D^0 = 1 \times 10^{-4} \text{ mol} \cdot \text{dm}^{-3}$ .	70
Figure 4.11	Combined representation of Job's plot for equimolar mother solutions of ARS and CTAB in water at 298K	70
Figure 4.12	Plot of absorbance Vs. wavelength of different volume fractions of the complex when $C_S^0 = 3 \times 10^{-4} \text{ mol} \cdot \text{dm}^{-3}$ and $C_D^0 = 3 \times 10^{-5} \text{ mol} \cdot \text{dm}^{-3}$	72
Figure 4.13	Job's plot for nonequimolar mother solutions of CTAB and ARS in water at 298 K. $C_S^0 = 3 \times 10^{-4} \text{ mol} \cdot \text{dm}^{-3}$ , $C_D^0 = 3.0 \times 10^{-5} \text{ mol} \cdot \text{dm}^{-3}$	74
Figure 4.14	Plot of Absorbance Vs wavelength of different volume fractions of the complex when $C_S^0 = 3 \times 10^{-4} \text{ mol} \cdot \text{dm}^{-3}$ and $C_D^0 = 6 \times 10^{-5} \text{ mol} \cdot \text{dm}^{-3}$	75
Figure 4.15	Job's plot for nonequimolar mother solutions of CTAB and ARS in water at 298 K. $C_S^0 = 3 \times 10^{-4} \text{ mol} \cdot \text{dm}^{-3}$ , $C_D^0 = 6.0 \times 10^{-5} \text{ mol} \cdot \text{dm}^{-3}$	77
Figure 4.16	Plot of Absorbance Vs. wavelength of different volume fractions of the complex when $C_S^0 = 3 \times 10^{-4} \text{ mol} \cdot \text{dm}^{-3}$ and $C_D^0 = 8 \times 10^{-5} \text{ mol} \cdot \text{dm}^{-3}$	78
Figure 4.17	Job's plot for nonequimolar mother solutions of CTAB and ARS in water at 298 K. $C_S^0 = 3 \times 10^{-4} \text{ mol} \cdot \text{dm}^{-3}$ , $C_D^0 = 8.0 \times 10^{-5} \text{ mol} \cdot \text{dm}^{-3}$	80
Figure 4.18	Plot of equilibrium complex formation constant ( $K_{eq}$ ) in water Vs. the mother solution concentrations of ARS at 298 K	81
Figure 4.19	Plot of absorbance Vs. wavelength of different volume fractions of the complex at 20°C	82
Figure 4.20	Job's plot for nonequimolar mother solutions of ARS and CTAB in water at 20°C	84
Figure 4.21	Plot of absorbance Vs. wavelength of different volume fractions of the complex at 25°C	85
Figure 4.22	Job's plot for nonequimolar mother solutions of ARS and CTAB in water at 25°C	87
Figure 4.23	Absorption spectra of different volume fractions of the complex at 30°C	88

Figure No	Caption	Page No
Figure 4.24	Job's plot ( $\Delta A$ Vs. $X$ ) of the complex in water at 30°C	89
Figure 4.25	Absorption spectra of different volume fractions of the complex at 35°C	90
Figure 4.26	Job's plot ( $\Delta A$ vs. volume fraction of surfactant solution) for the complex in water at 35°C	92
Figure 4.27	Plot of absorbance VS wavelength of the different volume fractions of the complex at 40°C	93
Figure 4.28	Job's plot for the complex in water at 40°C	95
Figure 4.29	Van't Hoff Plot for the electrostatic complex between ARS and CTAB in aqueous medium	97
Figure 4.30	FTIR spectrum of CTAB	102
Figure 4.31	FTIR spectrum of ARS	104
Figure 4.32	FTIR spectrum of ARS-CTAB complex in aqueous medium	105
Figure 4.33	Possible mechanism of the interaction between ARS and CTAB	106

The surfactants are drawing the attention of analytical chemists in recent years, due to their uses in analytical methods which provide an increase in selectivity and sensitivity. Surfactants increase the solubility of organic compounds in water and also catalyse some reaction, modifying the micro-environment in which the reactants are produced [1]. Studies of dye-surfactant interactions provide useful information for industrial applications since surfactants are used to assist in dyeing by wetting and leveling or by dispersing dyes of low solubility. Their interactions with dyes play a very important role in achieving level dyeing by assisting in wetting textiles and by controlling dye absorption by fibers [2].

Dye-surfactant interactions are interesting for their complex nature [1, 2, 3, 4]. The nature and mechanism of interactions of surfactants with chemical systems are still not clearly understood [1]. These interactions depend mostly on the chemical structure of these compounds [5, 6, 7]. Spectral changes of many cationic dyes caused by the presence of ionic surfactants and the dependence of such changes on surfactant concentration have been well studied [3, 8, 9].

Molecular complexes having characteristic physicochemical features may be formed at concentrations below the critical micelle concentration (CMC). If a surfactant is added to such a dye solution at submicellar concentrations, both the surfactant monomer and the dye aggregate can interact. Electrostatic interactions and /or hydrophobic interactions may take place [1]. The existence of ion-

association complex at concentrations below the CMC between the ionic surfactants and dyes with opposite charge supported by most published data. They have stoichiometric surfactant /dye ratios [1, 2, 4].

It appears that at premicellar surfactant concentrations very complex dye-surfactants aggregates are formed. At the postmicellar concentrations the aggregates are ruptured into dye monomers incorporating into the micelles. Spectral changes are observed when oppositely charged surfactants dyes are interacted in the premicellar region. These spectral changes are attributed to the formation of different chemical species. Various attempts have been made to determine the chemical composition of these complexes like Principal component analysis method [3] and the method of continuous variations, also called Job's method [2].

The method of continuous variations also called Job's method is commonly used to determine the composition of complexes in solution. The method was originally described by Ostromisslensky in 1911 and principles were outlined by Dension in 1912, but generally it is ascribed to Paul Job, who published in 1928 a detailed application of the method to the study of a wide range of coordination compounds. Job's method is capable of yielding both the stoichiometric composition and the association constant of the complex where a measured experimental property is a linear function of the concentration and where only one complex is important [10, 11]. Spectrophotometric measurements are very suitable for applications of Job's method, because light absorption is proportional to the concentration of the absorbing species, which is one of the necessary

conditions for quantification. In a similar study Sinem Gokturk and Melda Tuncay examined the interaction of cationic dye Safranin-O (SO) with anionic surfactant [sodium dodecylsulfonate (SDSO) and Sodium dodecylsulfate (SDS) in the premicellar region far below the critical micelle concentration in aqueous medium using the method of continuous variations or Job's method [2].

## **Aims and Objectives**

The aims and objectives of my project includes

- o To study the interactions b/w An anionic anthraquinoid dye Alizarin Red S and a cationic surfactant Cetyltrimethylammonium Bromide in the premicellar region in aqueous medium spectrophotometrically
- o To apply Job's Method also called The method of continuous variations to study the complexation or the ion-pair association phenomenon at the low surfactant concentration
- o To determine the equilibrium complex formation constant at room temperature
- o To study the effect of temperature on the equilibrium complex formation constant
- o To calculate the various thermodynamic parameters like  $\Delta G$ ,  $\Delta H$  and  $\Delta S$
- o To suggest the possible mechanism of these interactions



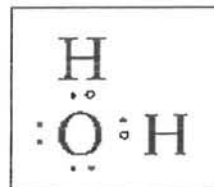
## CHAPTER-2

### THEORATICAL BACKGROUND

---

#### Part-I

#### 2.1 The Anomalous Properties of Water



Before discussing surfactants and water-soluble products, a brief review of some of the properties of water might be advisable. From a practical consideration, water is used in chemical processing and in product formulations because it is abundant and cheap. Several of the important properties of water can be summarised as follows:

- Water is a good solvent.
- Water has a relatively high boiling point (100°C) or 212°F at 760mm Hg).
- Water is stable.
- Water is a common reaction media for neutralisation and hydrolysis reactions.

These properties are based on water being strongly associated and polar in nature.

Water is relatively stable chemically. It ionises only slightly, but will hydrolyse or react with a number of materials. It is stable at very high temperatures. Many reactions are catalysed by the addition of very small amounts of water, with corrosion or rust being an outstanding example.

An important property related to the internal attraction or association of molecules in a liquid is called surface tension. Water has many unusual properties as a result of its ability to hydrogen bond. For example, the density of ice is less than that of the liquid and the predicted boiling point is almost 200 degrees C higher than it would be without hydrogen bonding. The water molecules at the surface of water are surrounded partially by air and partially by water. These surface molecules would be much more stable if they could be in the interior of the liquid where all their hydrogen bonds could be fulfilled (cohesion). Therefore, water normally tends to have the smallest surface possible, i.e. it has a high surface tension, in order to achieve the lowest possible energetic state.

Water has an extremely low isothermal compressibility and is a poor solvent for apolar compounds. The latter property of water has led to the term “hydrophobicity”, although this description might seem somewhat deceptive since London dispersion interactions between water and apolar solutes are favorable and quite marked [13]. Hydrophobic effects play an important role in many biochemical processes in aqueous solution like protein folding, molecular recognition processes, aggregation of amphiphilic molecules and surface forces [14]. In studies on hydrophobic effects, two phenomena are usually distinguished: hydrophobic hydration and hydrophobic interactions [14].

## **2.2 Hydrophobic Hydration**

The term hydrophobic hydration refers to the interactions of apolar solutes and water, i.e., how an apolar solute affects the water structure in its immediate environment [14]. Introduction of an apolar solute into aqueous solution is characterized by an unfavorable change in standard Gibbs energy at room temperature. However, the standard enthalpy of

the solution process is usually small and favorable whereas the entropy change is large and negative [15, 16, 17].

### **2.3 Hydrophobic Interactions**

The term “hydrophobic interactions” refers to the tendency of apolar molecules to stick together in aqueous solution [14]. These interactions play an important role in many biochemical processes like protein folding and the formation of lipid membranes. Kauzmann introduced the concept of hydrophobic interactions in 1959 [18]. He explained the entropy gain upon interaction of apolar compounds by the release of structured water molecules by destructive overlap of hydrophobic hydration shells. Hydrophobic interactions have been classified into pair wise and bulk interactions. Pair wise hydrophobic interactions are 1:1 interactions between individually hydrated nonpolar particles in aqueous solution where the solute concentration is below the so-called critical aggregation concentration. At these concentrations aggregation of solutes is hampered by the surrounding hydration shell; actually, “apolar solutes are screened when compared to the gas phase” [14]. In aqueous solution, pair wise hydrophobic interactions occur via “hydrophobic encounters” indicating that the molecules only associate transiently. Premicellar aggregation occurs at concentrations far below the critical aggregation concentration of the individual solutes [19].

### **2.4 Surfactants**

Surfactants are wetting agents that lower the surface tension of a liquid, allowing easier spreading, and lower the interfacial tension between two liquids. The term *surfactant* is a blend of “surface acting agent”. Surfactants are usually organic compounds that are amphiphilic, meaning they contain both hydrophobic groups (their “tails”) and

hydrophilic groups (their "heads"). Therefore, they are soluble in both organic solvents and water. The term surfactant was coined by Antara Products in 1950. Surfactants are among the most versatile of the products of the chemical industry, the pharmaceutical, the detergents, the drilling mud and the flotation agent. Of late, surfactants have become the subject of intense investigation by researchers in the fields of chemical kinetics and biochemistry because of the unusual properties of the polymeric forms (micelles) of these materials. Surfactant or surface active agent is a substance that, when present at low concentration in a system, has the property of adsorbing onto the surfaces or interfaces of the system and of altering to a marked degree the surface or interfacial free energies of those surfaces [20]. Surfactants are also referred to as wetting agents and foamers. Surfactant lowers the surface tension of the medium in which it is dissolved. By lowering this interfacial tension between two media or interfaces (e.g. air/water, water/stain, stain/fabric) the surfactant plays a key role in the removal and suspension of dirt. The lower surface tension of the water makes it easier to lift dirt and grease off of dirty dishes, clothes and other surfaces, and help to keep them suspended in the dirty water. The hydrophilic head remains in the water and it pulls the stains towards the water, away from the fabric. The surfactant molecules surround the stain particles, break them up and force them away from the surface of the fabric. They then suspend the stain particles in the wash water to remove them.

Surfactants have a vital role to play in preventing the re-deposition of soils like greasy, oily stains and particulate dirt on the surface or fabric from which they have just been removed. This works by electrostatic interactions and steric hindrance.

**(i) Electrostatic interactions**

Anionic surfactants are adsorbed on both the surface of the dirt which is dispersed in the detergent solution, and the fabric surface. This creates a negative charge on both surfaces, causing electrostatic repulsions. This repulsion prevents the soil from re-depositing on the fabric.

**(ii) Steric hindrance**

Non-ionic surfactants like alcohol ethoxylates also adsorb on the dirt. Their long ethoxylated chains extend in the water phase and prevent the dirt droplets or particles from uniting, and from depositing onto the fabric surface. This is shown in the illustration below: (1) Dirt is present in solution (2) The non-ionic surfactants adsorb to the dirt particles. (3) Their long hydrophilic heads extend in the water phase and as a result prevent the dirt particles/droplets from uniting and from re-depositing onto fabrics.

**2.4.1 Surfactants of natural and synthetic origin**

They can be either. Surfactants from natural origin (vegetable or animal) are known as oleo-chemicals and are derived from sources such as palm oil or tallow. Surfactants from synthetic origin are known as petro-chemicals and are derived from petroleum.

Surfactants also have an important role in our body, where they are used to reduce surface tension in the lungs. The human body does not start to produce lung surfactants until late in foetal development. Therefore, premature babies are often unable to breathe properly, a condition called Respiratory Distress Syndrome. Untreated, this is a serious illness and is often fatal, but administration of artificial surfactants virtually eliminates this health problem.

## 2.4.2 Structure of Surfactant

A surfactant consists of a hydrophobic (non-polar) hydrocarbon "tail" and a hydrophilic (polar) "head" group. The specific structure of the surfactant consisting of polar and non polar group is the basis of the inherent properties of the surfactants such as;

- o Adsorption at the interfaces
- o Lowering of surface tension
- o Self-association in bulk
- o Formation of organised molecular assemblies or supramolecular structures

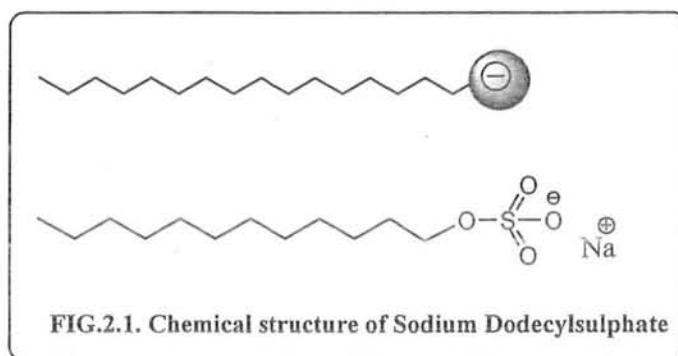
## 2.4.3 Classification of Surfactants

Surfactants may be classified according to their applications (emulsifiers, foaming agents, wetting agents, dispersants, etc), some physical characteristics (water or oil solubility and stability) and chemical structure of the material (type of linking group between the hydrophile and hydrophobe). The most useful chemical classification of surface active agents is based on the nature of the hydrophile, with subgroups being defined by the nature of the hydrophobe. Depending on the nature of the hydrophilic group, surfactants are classified into four groups [20]. Surfactants are said to fall into four broad categories: anionic, cationic, nonionic, and zwitterionic.

### (i) Anionic Surfactants

In solution, the head is negatively charged. This is the most widely used type of surfactant for laundering, dishwashing liquids and shampoos because of its excellent cleaning properties. The surfactant is particularly good at keeping the dirt away from

from fabrics, and removing residues of fabric softener from fabrics. Anionic surfactants are particularly effective at oily soil cleaning and oil/clay soil suspension. Still, they can react in the wash water with the positively charged water hardness ions (calcium and magnesium), which can lead to partial deactivation. The more calcium and magnesium molecules in the water, the more the anionic surfactant system suffers from deactivation. The most commonly used anionic surfactants are alkyl sulphates, alkyl ethoxylate sulphates and soaps.



## (ii) Cationic surfactant

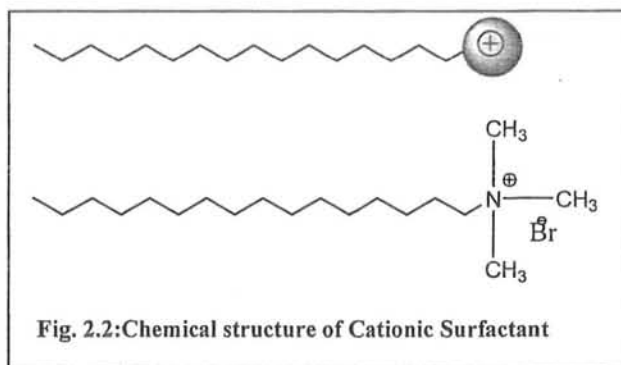
In solution, the head is positively charged. There are 3 different categories of cationics each with their specific application:

(i) In fabric softeners and in detergents with built-in fabric softener, cationic surfactants provide softness.

(ii) In laundry detergents, cationic surfactants (positive charge) improve the packing of anionic surfactant molecules (negative charge) at the stain/water interface. This helps to reduce the dirt/water interfacial tension in a very efficient way, leading to a more robust

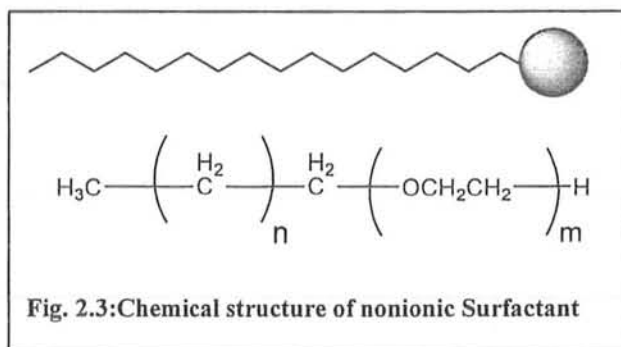
dirt removal system. They are especially efficient at removing greasy stains.

(iii) In household and bathroom cleaners, cationic surfactants contribute to the disinfecting/sanitizing properties.



### (iii) Non-ionic surfactants

These surfactants do not have an electrical charge, which makes them resistant to water hardness deactivation. They are excellent grease removers that are used in laundry products, household cleaners and hand dishwashing liquids. Most laundry detergents contain both non-ionic and anionic surfactants as they complement each other's cleaning action. Non-ionic surfactants contribute to making the surfactant system less hardness sensitive. The most commonly used non-ionic surfactants are ethers of fatty alcohols.

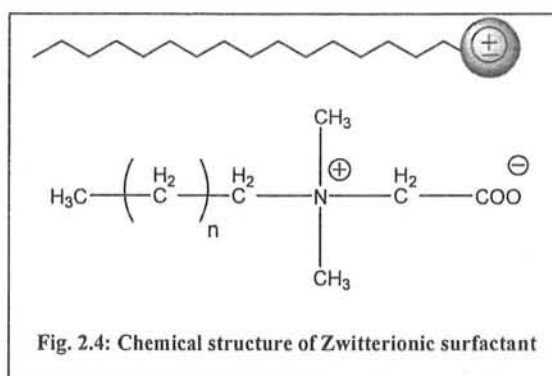




#### (iv) Amphoteric/zwitterionic surfactants

These surfactants are very mild, making them particularly suited for use in personal care and household cleaning products. They can be anionic (negatively charged), cationic (positively charged) or non-ionic (no charge) in solution, depending on the acidity or pH of the water. They are compatible with all other classes of surfactants and are soluble and effective in the presence of high concentrations of electrolytes, acids and alkalis.

These surfactants may contain two charged groups of different sign. Whereas the positive charge is almost always ammonium, the source of the negative charge may vary (carboxylate, sulphate, sulphonate). These surfactants have excellent dermatological properties. They are frequently used in shampoos and other cosmetic products, and also in hand dishwashing liquids because of their high foaming properties.  $\text{RN}^+\text{H}_2\text{CH}_2\text{COO}^-$  (long chain amino acid) and  $\text{RN}^+(\text{CH}_3)_2\text{CH}_2\text{CH}_2\text{SO}_3^-$  (sulphobetain) are examples of zwitterionic surfactants.



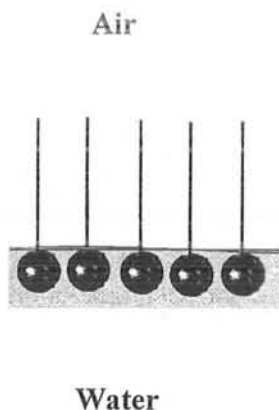
#### 2.4.4 Properties of Surfactants

The amphiphilic structure of surfactants suggests unusual properties, leading to both widespread and highly specialized applications. There are two main properties of surfactants: adsorption and self-assembly.

##### *(i) Adsorption*

One of the characteristic features of surfactants is their tendency to adsorb at interfaces in an oriented fashion. Since surface activity depends on the structure of the surfactant, and the solvent, temperature, and other conditions of use, the effect of these variations on the adsorption of surfactants at various interfaces has been studied extensively. This adsorption has been studied to determine (1) the concentration of surfactant ions at the interface, since this is a measure of how much of the interface has been covered (and thus changed) by the surfactant; the performance of the surfactant in many interfacial processes (e.g., foaming, detergency, emulsification) depends on its concentration at the interface; (2) the orientation of the surfactant at the interface, since this determines how the interface will be affected by the adsorption; that is, whether it will become more hydrophilic or more hydrophobic; (3) the energy change in the system,  $\Delta G$ ,  $\Delta H$ , and  $\Delta S$ , resulting from the adsorption, since these quantities provide information on the type and mechanism of any interactions involving the surfactant at the interface and the efficiency of its operation as a surface-active material. The adsorption properties of surfactants mean that surfactant molecules are usually found at the interface between an oil phase and a water phase or a water phase and an air phase. Thus this molecular property leads to the

macroscopic properties of wetting, foaming, detergency and emulsion formation.



Surfactant molecules tend to adsorb to the surface of oil droplets. The hydrophilic heads stick out into the water phase, while the hydrophobic tails happily stick into the oil phase.

#### (ii) *Self-Assembly*

Self-assembly is the tendency for surfactant molecules to organize themselves into extended structures in water. This includes the formation of micelles, bilayers and liquid crystals. These structures are formed by when the hydrophobic tails of the surfactants cluster together, forming small aggregates such as micelles, or large layer structures (bilayers), which are similar to a cell wall.

Surfactants also aggregate to form extended structures in water, such as the surfactant bilayer.

### **2.5 Aggregation behavior of surfactants**

A micelle (rarely micella, plural micelles) is an aggregate of surfactant molecules dispersed in a liquid colloid. A typical micelle in aqueous solution forms an aggregate with the hydrophilic "head" regions in contact with surrounding solvent, sequestering the

hydrophobic tail regions in the micelle centre. This type of micelle is known as a normal phase micelle (oil-in-water micelle). Inverse micelles have the headgroups at the centre with the tails extending out (water-in-oil micelle). Micelles are approximately spherical in shape. Other phases, including shapes such as ellipsoids, cylinders, and bilayers are also possible. The shape and size of a micelle is a function of the molecular geometry of its surfactant molecules and solution conditions such as surfactant concentration, temperature, pH, and ionic strength. The process of forming micellae is known as micellisation and forms part of the phase behaviour of many lipids according to their polymorphism.

### **2.5.1 Energy of formation of Micelles**

Micelles only form when the concentration of surfactant is greater than the critical micelle concentration (CMC), and the temperature of the system is greater than the critical micelle temperature, or Krafft temperature. The formation of micelles can be understood using thermodynamics: micelles can form spontaneously because of a balance between entropy and enthalpy. In water, the hydrophobic effect is the driving force for micelle formation, despite the fact that assembling surfactant molecules together reduces their entropy. Broadly speaking, above the CMC, the entropic penalty of assembling the surfactant molecules is less than the entropic penalty of caging the surfactant monomers with water molecules. Also important are enthalpic considerations, such as the electrostatic interactions that occur between the charged parts of surfactants.

## 2.5.2 Critical Micelle Concentration

In chemistry, the critical micelle concentration (CMC) is defined as the concentration of surfactants above which micelles are spontaneously formed. Upon introduction of surfactants (or any surface active materials) into the system they will initially partition into the interface, reducing the system free energy by a) lowering the energy of the interface (calculated as area x surface tension) and b) by removing the hydrophobic parts of the surfactant from contacts with water. Subsequently, when the surface coverage by the surfactants increases and the surface free energy (surface tension) has decreased, the surfactants start aggregating into micelles, thus again decreasing the system free energy by decreasing the contact area of hydrophobic parts of the surfactant with water. Upon reaching CMC, any further addition of surfactants will just increase the number of micelles (in the ideal case).

Phillips [21] defined CMC as “the concentration at which the properties of the surfactant solution change in the most abrupt manner”.

$$\left( \frac{d^3 \varphi}{dT_c^3} \right)_{T_c = CMC} = 0$$

Where  $\varphi$  is any physical property which varies linearly with the concentration of solution. It is generally the concentration of solutes at which the concentration of micelle would be zero.

### 2.5.3 CMC Measurements

Breaks in the electric conductivity, surface tension and light scattering or refractive index curves have been used most commonly for CMC measurements.

#### (i) Surface Tension Method

The critical micelle formation concentration (CMC) can be determined by carrying out surface tension measurements on a series of different surfactant concentrations. Surfactants exhibit a specific surface tension curve as a function of the concentration. Initially the surfactant molecules increasingly enrich themselves at the water surface. During this phase the surface tension decreases linearly with the logarithm of the surfactant concentration. When the CMC is reached, i.e. when the surface is saturated with surfactant molecules, a further increase in surfactant concentration no longer has any appreciable influence on the surface tension.

This means that in order to determine the CMC the two linear sections formed by the measuring points obtained from the series of different concentrations must be determined. The CMC is obtained from the intersection of the straight lines for the linear concentration-dependent section and the concentration-independent section.

#### (ii) Electric Conductivity

The sudden change in a measured property is interpreted as indicating a significant change in the nature of the solute species affecting the measured quantity. The conductivity  $\kappa$  of the solution decreases at the CMC owing to lower mobility of the larger micelles. Dividing by concentration to convert it to equivalent conductivity, gives a sharp reduction in the quantity at CMC, which is associated with an increase in mass per unit

charge of the conducting species.

### (iii) Osmotic Pressure

In the case of variation of osmotic pressure,  $\pi$  with concentration to a first approximation we have a relation as:

$$\frac{\pi}{RTc} = \frac{1}{M_2} + \frac{1}{2} \frac{\overline{B'} \overline{V}_1}{M_2^2} c = \frac{1}{M_2} + Bc$$

Where  $\overline{V}_1$  partial molar volume of solvent, B is the cluster of constants arises from the conversion of practical concentration units to the mole fraction and c represents the concentration in terms of mass volume<sup>-1</sup>. According to this equation, slope of a plot of this  $\pi$  verses c is proportional to  $1/M$  where M is molecular weight. Osmotic pressure measurements generally give the number of molecular weight  $M_n$ . In case of micellar solution, osmometry leads to weight average molecular weight  $\overline{M}_w$ . The decrease in the slope of the osmotic pressure at CMC indicates an increase in the average molecular weight of the solute at that point.

### (iv) Light Scattering

For light scattering, the change in the solution turbidity at CMC indicates the appearance of a scattering species of significantly greater size than the monomeric solute. In this case the slope is inversely proportional to M according to relation:

$$\frac{Hc}{\tau} = \frac{1}{M} + 2Bc$$

Where  $\tau$  is the turbidity,  $H$  is constant and  $c$  is concentration in terms of mass volume<sup>-1</sup>. The slope of a plot of  $\pi$  versus  $c$  is proportional to  $M$ . The break in the curve with increasing concentration corresponds to an increase in the molecular weight of the solute in solution at CMC.

#### 2.5.4 Factors Affecting CMC in Aqueous Solution

Among the factors known to affect the CMC markedly in aqueous solutions are:

- *Structure of the surfactant*
- *Presence of added electrolytes*
- *Presence of organic additives*
- *Temperature of the solution*

#### 2.5.5 Solubilization

One of the most important properties of aqueous micellar solution that is directly related to micelle formation is solubilization. Solubilization may be defined as the spontaneous dissolving of a substance by the reversible interaction with the micelle of a surfactant in a solvent to form a thermodynamically stable isotropic solution with reduced thermodynamic activity of the solubilized material. Solvent-insoluble materials may be dissolved by the solubilization mechanism; the importance of the phenomena from the practical point of view is that it makes possible the dissolving of substances in solvents in which they are normally insoluble. In solubilization, the solubilized material is in the same phase as the solubilizing solution, and the system is consequently thermodynamically stable.



### 2.5.6 Locus of Solubilization

The exact location of solubilization in the micelle varies with the nature of the material and it reflects the type of interaction occurring between surfactant and solubilization. Based on different studies [14], solubilization is believed to occur at a number of different sites in the micelle. (1) One is the surface of micelle at the micelle solvent interface. (2) Between the hydrophilic head groups. (3) In the so called palisade layer of the micelle between the hydrophilic ground and the first few carbon atoms of the hydrophobic groups that comprise the hydrophobic core of the micellar interior. (4) More deeply in the palisade layer. (5) In the inner core of the micelle.

Ionic micelles ordinarily have an extensive hydrophobic core region, which can interact strongly with hydrocarbon and halogenated hydrocarbon groups of solutes. Hydrophobic effects have often been considered to be dominant in determining the locus of solubilization [22, 23] but the effects of electrostatic interactions are also considered in relation to the solubilization of organic solutes in the ionic micelles.

### 2.5.7 Factors Affecting Solubilization

- Effect of Structure of Solubilizer
- Effect of Structure of Solubilize
- Effect of Electrolyte
- Effect of Temperature
- Effect of Organic Additives

## **Part-II**

### **2.6 Dyes**

A dye can generally be described as a colored substance that has an affinity to the substrate to which it is being applied. The dye is generally applied in an aqueous solution, and may require a mordant to improve the fastness of the dye on the fiber. Both dyes and pigments appear to be colored because they absorb some wavelengths of light preferentially. In contrast with a dye, a pigment generally is insoluble, and has no affinity for the substrate. Some dyes can be precipitated with an inert salt to produce a lake pigment, and based on the salt used they could be aluminum lake, calcium lake or barium lake pigments. Archaeological evidence shows that, particularly in India and the Middle East, dyeing has been carried out for over 5000 years. The dyes were obtained from animal, vegetable or mineral origin, with no or very little processing. By far the greatest source of dyes has been from the plant kingdom, notably roots, berries, bark, leaves and wood, but only a few have ever been used on a commercial scale.

#### **2.6.1 Classification of Dyes**

Dyes may be classified according to their structures or, alternatively, according to the methods by which they are applied to the substrate i.e., in dyeing and printing textiles, leather and fur dyeing, in paper manufacture, in mass coloration of plastics and as paints and surface coatings. Dyes may be classified in accordance with their chemical constitution or their application to textile fibers and for their coloring purposes.

Chromophores are essential color-producing groups, but color constitution relationships may be extremely complex; and for a systematic treatment of the chemistry of dyes a classification based primarily on characteristic structural units is more satisfactory. The azo group, the anthraquinone nucleus, and heterocyclic ring systems are examples of structural units, which provide a simple basis of division and subdivision.

### **2.6.1.1 Classification Of Dyes On The Basis Of mode Of Action**

#### **(i) Acid dyes**

These are water-soluble anionic dyes that are applied to fibers such as silk, wool, nylon and modified acrylic fibers using neutral to acid dyebaths. Attachment to the fiber is attributed, at least partly, to salt formation between anionic groups in the dyes and cationic groups in the fiber. Acid dyes are not substantive to cellulosic fibers. Most synthetic food colors fall in this category

#### **. Health and safety**

Any dyes including acid dyes have the ability to induce sensitisation in humans due to their complex molecular structure and the way in which they are metabolised in the body. This is extremely rare nowadays as we have a much greater understanding through experience and knowledge of dyestuffs themselves. Some acid dyes are used to colour food. We wear fabrics every day exposing our skin to dyes. The greatest risk of disease or injury due to dyes is by ingestion or exposure to dye dust. These scenarios are normally confined to textile workers. Whereby the dye itself is normally non toxic, the molecules are metabolised (usually in the liver) where they may be broken back down to the

original intermediates used in manufacture. Thus many intermediate chemicals used in dye manufacture have been identified as toxic and their use restricted.

#### **(ii) Basic dyes**

These are water-soluble cationic dyes that are mainly applied to acrylic fibers, but find some use for wool and silk. Usually acetic acid is added to the dye bath to help the uptake of the dye onto the fiber. Basic dyes are also used in the coloration of paper.

#### **(iii) Direct or substantive dyeing**

is normally carried out in a neutral or slightly alkaline dyebath, at or near boiling point, with the addition of either sodium chloride (NaCl) or sodium sulfate (Na<sub>2</sub>SO<sub>4</sub>). Direct dyes are used on cotton, paper, leather, wool, silk and nylon. They are also used as pH indicators and as biological stains.

#### **(iv) Mordant dyes**

These dyes require a mordant, which improves the fastness of the dye against water, light and perspiration. The choice of mordant is very important as different mordants can change the final color significantly. Most natural dyes are mordant dyes and there is therefore a large literature base describing dyeing techniques. The most important mordant dyes are the synthetic mordant dyes, or chrome dyes, used for wool; these comprise some 30% of dyes used for wool, and are especially useful for black and navy shades. The mordant, potassium dichromate, is applied as an after-treatment. It is important to note that many mordants, particularly those in the heavy metal category, can be hazardous to health and extreme care must be taken in using them.

**(v) Vat dyes**

These dyes are essentially insoluble in water and incapable of dyeing fibres directly. However, reduction in alkaline liquor produces the water soluble alkali metal salt of the dye, which, in this leuco form, has an affinity for the textile fibre. Subsequent oxidation reforms the original insoluble dye. The color of denim is due to indigo, the original vat dye.

**(vi) Reactive dyes**

These dyes utilize a chromophore attached to a substituent that is capable of directly reacting with the fibre substrate. The covalent bonds that attach reactive dye to natural fibers make them among the most permanent of dyes. "Cold" reactive dyes, such as Procion MX, Cibacron F, and Drimarene K, are very easy to use because the dye can be applied at room temperature. Reactive dyes are by far the best choice for dyeing cotton and other cellulose fibers at home or in the art studio.

**(vii) Disperse dyes**

These dyes were originally developed for the dyeing of cellulose acetate, and are substantially water insoluble. The dyes are finely ground in the presence of a dispersing agent and then sold as a paste, or spray-dried and sold as a powder. Their main use is to dye polyester but they can also be used to dye nylon, cellulose triacetate, and acrylic fibres. In some cases, a dyeing temperature of 130 °C is required, and a pressurised dyebath is used. The very fine particle size gives a large surface area that aids dissolution to allow uptake by the fibre. The dyeing rate can be significantly influenced by the choice of dispersing agent used during the grinding.

**(viii) Azoic dyes**

Azo dyeing is a technique in which an insoluble azoic dye is produced directly onto or within the fibre. This is achieved by treating a fibre with both diazoic and coupling components. With suitable adjustment of dyebath conditions the two components react to produce the required insoluble azo dye. This technique of dyeing is unique, in that the final color is controlled by the choice of the diazoic and coupling components.

**(ix) Sulfur dyes**

These are two part "developed" dyes used to dye cotton with dark colors. The initial bath imparts a yellow or pale chartreuse color. This is aftertreated with a sulfur compound in place to produce the dark black we are familiar with in socks for instance. Sulfur Black 1 is the largest selling dye by volume.

**(x) Metal complex dyes**

These dyes are produced as metal complexes of o'o-dihydroxy-azo dyes in bulk for use by the dyers as acid dyes mainly for wool; they also find application on silk and polyamide fiber. The dyes are of two kinds;

- Acid dyeing premetallized dyes (1 metal atom, usually chromium combined with one molecule of azo dyes) known as 1:1 dyes. The chief use is in wool dyeing but the large amount of sulfuric acid needed in the dye bath is often a disadvantage.
- Neutral dying premetallized dyes are much the more important type. They are 1:2 complexes (1 metal atom, chromium or cobalt combined with two molecules of azo dye).

*(xi) Solvent Dyes*

These dyes usually contain no sulpho or other water solubilizing groups, are soluble in organic solvents the nature of which varies according to application. The range of solvents covers alcohols, esters, aliphatic and aromatic hydrocarbons, oils, fats and waxes. Uses for the dye solutions include stains, varnishing and printing inks, copying papers, typewriter ribbons and ballpoint pens.

**2.6.1.2 Food dyes**

One other class which describes the role of dyes, rather than their mode of use, is the food dye. Because food dyes are classed as food additives, they are manufactured to a higher standard than some industrial dyes. Food dyes can be direct, mordant and vat dyes, and their use is strictly controlled by legislation. Many are azoic dyes, although anthraquinone and triphenylmethane compounds are used for colors such as green and blue. Some naturally-occurring dyes are also used. Synthetic food dyes, long blamed for causing hyperactivity in children, may have a good side: some of them may protect against cancer.

**2.6.1.3 Other important dyes**

A number of other classes have also been established, including:

- Oxidation bases, for mainly hair and fur
- Leather dyes, for leather
- Fluorescent brighteners, for textile fibres and paper
- Carbene dyes, a recently developed method for coloring multiple substrates

#### 2.6.1.4 Natural dyes

Natural dyes are the colors, which are obtained from plants. These dyes are applied on the substances with the help of minerals or metal salts. The metal salts are alum (aluminum salt), iron or tin (called mordants).

#### 2.6.1.5 Chemical classification

By the nature of their chromophores, dyes are divided into:

- Acridine dyes, derivatives of acridine
- Anthraquinone dyes, derivatives of anthraquinone
- Azo dyes, based on -N=N- azo structure
- Cyanine dyes, derivatives of phthalocyanine
- Diazonium dyes, based on diazonium salts
- Nitro dyes, based on a -NO<sub>2</sub> nitro functional group
- Nitroso dyes, based on a -N=O nitroso functional group
- Quinone-imine dyes, derivatives of quinone

### 2.6.2 Application of Dyes

#### (i) *Textile Application*

Dyes are applied to textile fibers by two distinct processes dyeing and printing of which the former is much more extensively used. In dyeing, the fiber absorbs the dye from an aqueous solution or dispersion, and is more or less uniformly colored. The solution of the dye is the dye liquor or dye bath, and as the dyeing precedes the concentration of the dye increases in the fiber and decreases in the bath. Ultimately under favorable conditions, there is practically no dye in the dye bath, which is then said to be exhausted. The



uniformity of the dyeing (level dyeing) depends on the absorptive power of the fiber, the nature of the dye, and the conditions of dyeing.

(ii) *Non-Textile Application*

- Dyes may serve as titration indicators, food colorants and hair colorants
- Examples of other applications of colorants
  - Photographic
  - Spectral sensitizing
  - Dye-forming process
  - Dye-bleach process
  - Image-diffusion process
- Biological histology
  - Affinity chromatography
  - Biochemical assay
  - Drugs
- Electrical/electronic
  - Liquid crystal displays
  - Electrography
  - Solar energy conversion
  - Organic conductors

The dye studied in the present work includes Alizarin Red S, which belongs to vat dyes. Alizarin Red S is a derivative of alizarin, another dye, from which it is derived by sulphonation. It belongs to the class of anthraquinone. Alizarin red S is effective for

calcium in tissue sections [24, 25]. This dye could be used as electroactive probe for the determination of CTAB concentration below CMC in alkaline media by using AC Voltammetry [26]. Determination of proteins with Alizarin Red S by Rayleigh light scattering technique has also been developed [27].

## Part-III

### 2.7 Ultraviolet Visible Spectroscopy

When an electromagnetic radiation is passed through a material and absorption of energy over a range of frequencies is measured, the relationship between energy and frequency is given by:

$$\Delta E = h\nu$$

Where  $\Delta E$  is the difference in the energy between the ground state and the excited state of the molecule. When light is passed through a liquid sample the rotational motion of the molecule is more or less ceased and molecule vibrates only and gives electronic transitions with UV light.

Electronic transitions involve the promotion of  $\sigma$ ,  $\pi$  or  $n$  (non-bonding or lone pair) electron from their ground states to higher states. These processes require radiation in the relatively higher energy ultraviolet and visible portion of the spectrum. UV light disturbs only the electronic energy states, i.e., the molecule is excited from ground electronic state to some higher electronic state and vibrational levels remain unaffected by these transitions. The regions of the electronic spectrum and the type of transition, which occurs in, each is shown in Figure 2.5.

The wavelength at which absorption occurs depends upon how firmly the electrons are bound in the molecule. The electrons in a single covalent bond are tightly bound, and radiation of high energy and short wavelength is required for their excitation. e.g., alkanes which contain C-H and C-C bonds show no absorption over 160nm. This is  $\sigma \rightarrow \sigma^*$  transition. Electron in a double or triple bond are rather easily excited to the

higher pi orbital transition is designated as  $\pi \rightarrow \pi^*$  when a pi electron is raised from a pi-bonding orbital to a pi-antibonding orbital.

Most applications of UV and visible spectroscopy to organic compounds are based on  $n \rightarrow \pi^*$  and  $\pi \rightarrow \pi^*$  transitions and hence require the presence of chromophore groups in the molecule. These transitions occur in the region of the spectrum (about 200-700nm), which is convenient to use experimentally.

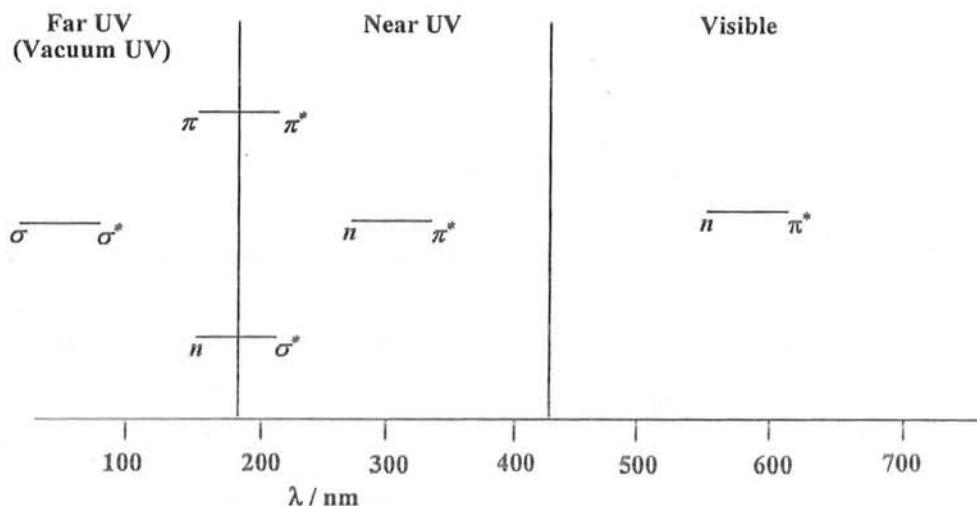


Fig. 2.5: Different transitions in UV-Visible region

As the dye used in present work contain conjugated double bonds, so it is possible to measure their absorption spectra using UV-visible spectroscopy the intensity of an electronic absorption is given by equation:

$$A = \log I_0 / I_t = \epsilon cl$$

Where A is the absorbance by the sample, c is the concentration of the sample ( $\text{mol dm}^{-3}$ ), l is the path length of the sample (cm),  $I_0$  is the intensity falling on the sample, and  $I_t$  is the intensity transmitted by the sample,  $\epsilon$  is the molar extinction coefficient ( $\text{dm}^3 \text{mol}^{-1} \text{cm}^{-1}$ ). The simple relation we obtained is:

$$A = \epsilon cl$$

It is obvious that absorbance  $A$ , is directly proportional to  $c$ , of the sample in the solution. This relationship is known as Beer-Lambert law. This states that the absorbance of a solution is directly proportional to the solution's concentration. Thus UV/VIS spectroscopy can be used to determine the concentration of a solution. It is necessary to know how quickly the absorbance changes with concentration. Because the absorbance of a sample will be proportional to the number of absorbing molecules

### **Limitations of Beer-Lambert law**

The linearity of the Beer-Lambert law is limited by chemical and instrumental factors.

Causes of nonlinearity include:

- deviations in absorptivity coefficients at high concentrations due to electrostatic interactions between molecules in close proximity
- scattering of light due to particulates in the sample
- fluorescence or phosphorescence of the sample
- changes in refractive index at high analyte concentration
- shifts in chemical equilibria as a function of concentration
- non-monochromatic radiation, deviations can be minimized by using a relatively flat part of the absorption spectrum such as the maximum of an absorption band
- stray light

### ***Chromophore***

Any structural feature present in a molecule that is responsible for absorption of electromagnetic radiations is known as chromophore. A covalently unsaturated group

responsible for electronic absorption e.g. C=C, C=O and NO<sub>2</sub>. The presence of chromophores in a molecule is best documented by UV-Visible spectroscopy, but the failure of most instruments to provide absorption data for wavelengths below 200 nm makes the detection of isolated chromophores problematic. Fortunately, conjugation generally moves the absorption maxima to longer wavelengths, as in the case of isoprene, so conjugation becomes the major structural feature identified by this technique. Thus, extending conjugation generally results in bathochromic and hyperchromic shifts in absorption.

The appearance of several absorption peaks or shoulders for a given chromophore is common for highly conjugated systems, and is often solvent dependent. This fine structure reflects not only the different conformations such systems may assume, but also electronic transitions between the different vibrational energy levels possible for each electronic state.

To understand why conjugation should cause bathochromic shifts in the absorption maxima of chromophores, we need to look at the relative energy levels of the pi-orbitals. When two double bonds are conjugated, the four p-atomic orbitals combine to generate four pi-molecular orbitals (two are bonding and two are antibonding). In a similar manner, the three double bonds of a conjugated triene create six pi-molecular orbitals, half bonding and half antibonding. The energetically most favorable  $\pi \rightarrow \pi^*$  excitation occurs from the highest energy bonding pi-orbital (**HOMO**) to the lowest energy antibonding pi-orbital (**LUMO**). Increased conjugation brings the HOMO and LUMO orbitals closer together. The energy ( $\Delta E$ ) required to effect the electron promotion is therefore less, and the wavelength that provides this energy is increased correspondingly,

### *Auxochrome*

A saturated group with nonbonding electrons which when attached to a chromophore alters both  $\lambda_{\text{max}}$  and intensity of absorption e.g. OH, NH and Cl.

### *Hypsochromic Shift*

The shift of absorption to a shorter wavelength due to substitution or solvent effect is called blue-shift or hypsochromic shift.

### *Bathochromic Shift*

The shift of absorption to a longer wavelength due to substitution or solvent effect is called red-shift or bathochromic shift.

### *Hyperchromic Shift*

Increase in absorption intensity.

### *Hypochromic Shift*

Decrease in absorption intensity

### **Applications Of UV-VISBLE Spectroscopy**

There are numerous applications of UV-VIS spectroscopy. Some of the most important applications of this spectroscopic technique are in:

- Structure determination
- Analytical applications
- Kinetic measurements
- Determination of ionization constants
- Stereochemical studies

## **Part IV**

### **2.8 Dye – Surfactant Complex Formation**

The phenomenon of dye- surfactant complexation has been proved by most published data in both premicellar [2, 3, 4, 6, 7, 12] and supermicellar region [1]. Surfactants contain both hydrophobic and hydrophilic part in their structure. Solution properties of dye solutions such as electrical conductivity and absorption spectrum are changed by the addition of small amounts of surfactant with varying the environment of the solution. The changes as a function of surfactant concentration in the measured quantities indicate a significant variation in the nature of the solution. When the charge of the surfactant is opposite of that of dye, the attractive forces between the dye and surfactant molecules lead to dye–surfactant complex formation in the solution [28].

Various techniques such as spectrophotometry [1], [2], [3],[4],[6] and [12] , conductometry [28, 29], potentiometry [30], and voltammetry [31] were used to understand the interactions between dyes and surfactants. These techniques have some advantages and disadvantages.

#### **2.8.1 Potentiometry**

Surfactant-selective membrane electrodes are used for the potentiometric methods. So, surfactant-selective electrodes should be prepared to study dye–surfactant interactions. Moreover, these electrodes work only in a specific concentration and pH ranges. These are disadvantages of potentiometric methods [28].

#### **2.8.2 Conductometry**

Conductometer is cheap equipment and conductometric method is also easy to investigate



the interactions between molecules. Conductance measurement proved to be a simple method for the detection of dye–surfactant ion pairs in an aqueous solution. As the specific conductivity of the individual species in the solution increased linearly with concentration, a gradual lowering of specific conductivity after a certain concentration of added surfactant indicates the formation of non-conducting species. The main drawback to conductometric investigations of dye–surfactant ion pair formation is that for a numerical description, namely the calculation of equilibrium constants, a suitable theoretical model is required and this can include certain simplifications [29].

### **2.8.3 Spectroscopic investigation of dye–surfactant ion pair formation in aqueous solution**

The most widely used technique for the determination of complexes formed between oppositely charged dyes and surfactants is spectroscopic technique [1, 6, 12]. Surfactants are able to affect the electronic absorption spectra of many dyes. Below the critical micelle concentration (CMC) a spectral change indicates a formation of complex between dye and surfactants. Spectral studies of methyl violet in aqueous solutions of different surfactants in supermicellar concentration region have been done by M.Sarkar, S.Poddar. The equilibrium constant is determined using the Scott equation, and also from Bensi Hildebrand equation [1].

Various methods have been applied for the determination of the chemical compositions and equilibrium complex constant of complexes so formed in the premicellar region, like the principal component analysis method, method followed by Vitagliano et al [3] and the method of continuous variation also called Job's method [10]. Job's method of

continuous variation is a commonly used procedure for determining the composition of complexes in solution. The popularity of this method is indicated by the frequency of its inclusion in a wide variety of analytical chemistry, instrumental analysis and advanced chemical equilibrium texts as well as its application in many research articles. The use of Job's method in the undergraduate laboratory has also been the subject of a number of publications. The principle of continuous variations was employed by Ostromisslensky in 1911 to establish the 1:1 stoichiometry of the adduct formed between the nitrobenzene and aniline. The principle was used by Denison in 1912 in a study of various liquid mixtures. However, the method of continuous variations is generally associated with the name of Job who in 1928 published a detailed application of the method to the study of a wide variety of coordination compounds.

Job's method as commonly practiced, is carried out in batch mode by mixing aliquots of two equimolar stock solutions of metal and ligands (sometimes followed by dilution to a fixed volume). These solutions are prepared in a manner such that total analytical concentration of metal plus ligand is maintained constant while the ligand:metal ratio varies from flask to flask, that is:

$$C_M + C_L = k$$

Where  $C_M$  and  $C_L$  are the analytical concentration of metal and ligand, respectively, and  $k$  is a constant. The absorbance, or more frequently the corrected absorbance, is plotted as a function of mole fraction of ligand or metal in the flasks. The resulting curves, called Job's plots, yield a maximum (or minimum) the position of which indicates the ligand:metal ratio of the complex in solution. For example, a maximum corresponding to 0.5 on the mole fraction of ligand scale suggests a complex of 1:1 composition, while

maxima at 0.67 and 0.75 indicate complexes of 2:1 and 3:1 ligand :metal ratio respectively. While absorbance is by far the most commonly employed property of the solution for measuring Job's plots, other solution properties can also be used.

Here two points need to be explained. First, the definition of corrected absorbance is somewhat unusual. It is defined as the measured absorbance (at a given wavelength) minus the sum of the absorbances which the metal and ligand would exhibit if no complexation has occurred. Mathematically, the corrected absorbance,  $Y$ , is defined as:

$$Y = A - (\epsilon_M C_M + \epsilon_L C_L) b$$

Where  $A$  is the measured absorbance,  $\epsilon_M$  and  $\epsilon_L$  are the absorptivities of metal and ligand, respectively, and  $b$  is the optical path length. Second the term mole fraction as used in this context is not the true mole fraction in that the solvent is omitted from its calculation.

The mole fraction of ligand  $\chi_L$ , is defined as:

$$\chi_L = \frac{C_L}{C_M + C_L}$$

And can evidently vary between zero and unity. Mole fraction of metal is similarly defined.

There are a number of requirements which must be satisfied in order for Job's method to be applicable. The first two requirements relate to the chemical behaviour of the system under investigation and the second two relate to how the experiment is actually carried out. These requirements are:

- 1) the system must confirm to Beer's law,
- 2) one complex must predominate under the conditions of the experiment,
- 3) the total concentration of metal plus ligand must be maintained constant, and
- 4) pH and ionic strength must be maintained constant

It is surprising that Job's method is frequently employed without first checking requirement. For sake of completeness, it is worth pointing out that there are variations of Job's method in which conditions (2) or (3) are not satisfied. Vosburgh and Cooper described an extension of Job's method which allows the composition of a series of complexes, formed in a stepwise fashion, to be established. However, this variation of Job's method is very limited in that its applicability is conditional upon a fortuitous combination of spectral differences and stepwise formation constants for the individual complexes. Consequently, the method of Vosburgh and Cooper is not generally applicable. In the second modification of Job's method condition 3 is not satisfied, that is, nonequimolar solutions are mixed. This modification is one of the techniques by which stability constants of complexes can be obtained from Job's plots. However, while Job's plots are frequently used for determining compositions, their use for determining stability constants has been severely criticized.

In measuring Job's plots, two experimental crosschecks are often recommended, though not always carried out, in order to evaluate the reliability of the data:

- 1) all readings should be carried out at more than one wavelength and
- 2) the complete experiment should be conducted at more than one metal-plus-ligand concentration. In order for the method to be applicable, the position of the maximum on the mole fraction axis must be invariant as a function of the changes recommended in crosschecks (1) and (2) above.

These important crosschecks are frequently overlooked in the application of Job's method [10]. The method of continuous variations or Job's method is one of the most common techniques used for complex ion studies. Where a measured experimental

property is a linear function of the concentration and where only one complex is important. Job's method is capable of yielding both the stoichiometric composition and the association constant of the complex. Continuous variation plots are the diagrams of a physical property, which is related to the concentration of an equilibrium two component complex against volume or mole fraction of one of the two constituents.

Spectrophotometric measurements are very suitable for the application of this method. Plots are prepared by mixing the solutions of individual components in varying volume ratios in such a way that the total volume of each mixture is the same. The absorbance of each mixed solution is measured and plotted against the volume fraction of one of the reactants. The resulting curve has a maximum or a minimum, the position of which shows the composition of the associate on the abscise. According to Job the stoichiometry of the complex is determined from equimolar diagrams, which are obtained from solutions of identical initial concentration, while to determine the equilibrium constant, a nonequimolar diagram, obtained of solutions of different initial concentration, must be plotted. This means that two series of measurements are needed. However equilibrium association constants ( $K$ ) can also be determined by two other methods, Schaeppi–Treadwell's and Schwarzenbach's, which are derived from Job's method. The stoichiometry and the stability of the associate can be determined by equimolar solutions by these modified methods, so the additional measuring of nonequimolar solutions is not necessary.

The method of Schaeppi and Treadwell is suitable when only one stable associate is formed and the equilibrium constant value is high. Schwarzenbach introduced a method, which is also valid for less stable associates, where Job's plots have no linear parts and an

exact relation between a slope of the curve and the equilibrium constant must be determined [11].

We have a spectroscopic study of the complex formed between the cationic surfactant cetyltrimethylammonium bromide and an anionic dye Alizarin Red S in aqueous media using Job's method. We have determined the chemical composition of the complex using equimolar mother solutions of both dye and surfactant and then calculated the equilibrium complex formation constant making use of nonequimolar mother solutions of both dye and surfactant. We also calculated equilibrium complex formation constant at different temperatures using same method. Different thermodynamic parameters like  $\Delta G$ ,  $\Delta H$ ,  $\Delta S$  are calculated.

## Part V

### 2.9 Literature Review

Dye-surfactant interactions have been widely studied via different techniques both in the premicellar and micellar regions.

Sinem Gokturk and Melda Tuncay studied the interaction of a cationic dye with anionic surfactants having same hydrophobic but different polar groups spectrophotometrically in the premicellar region far below the critical micelle concentration in aqueous media using Job's method. They observed strong interactions between the oppositely charged surfactants and the dye and reported 1:1 complex formation ratio. Using nonequimolar mother solutions of the dye and surfactants they calculated equilibrium composition constants [2].

M.Sarkar and S.Poddar studied the interactions of a cationic dye with ionic (cationic and anionic) and nonionic surfactants in the premicellar and micellar, and supermicellar regions spectrophotometrically. They observed strong interactions between the dye and anionic surfactant both in the premicellar and micellar concentration regions and an electrostatic interaction in the supermicellar region. With the nonionic surfactant the dye solubilizes in the micellar region while in the supermicellar region the dye forms 1:1 charge transfer complex with the nonionic surfactant. The dye acts as the electron acceptor and the surfactant as the electron donors. No interaction is observed between the dye and the cationic surfactant in premicellar, micellar and supermicellar regions. The binding constant calculated in the supermicellar concentration region at different temperatures indicates that binding between the dye and surfactant decreases with increasing temperature [1, 4].

Anil Kumar Mandal and Medini Kanta Pal had a spectroscopic study of the interaction between a cationic dye and an ionic surfactant in aqueous medium. They applied The Principal Component Analysis method to determine the composition as well as molar absorption coefficient of the complex. Further they applied the method followed by Vitagliano et al to determine the equilibrium constant [3].

Kerry K. Karukstis, Daniel A.Savin, Christine T. Loftus, and Noel D. D Angelo have spectroscopic study of the interaction of Azo dyes with cationic surfactants differing only in the number of carbon atoms in the alkyl chain and investigated the 1:1 ion pair complexes formed from electrostatic interaction of the cationic surfactants with the anionic organic probe in aqueous solution. Complex formation was evident by a blue shift observed in the  $\lambda_{\text{max}}$  of the Azo dye with increasing surfactant concentration. The ratio of the Azo dye to surfactant in the ion-pair complexes were verified by the method of continuous variation [6].

S.S.Shah, G.M. Laghari and K. Naeem studied the interaction of hemicyanine dyes with an anionic surfactant by absorption spectra as a function of surfactant concentration above and below critical micelle concentration. Red shift observed with increasing surfactant concentration in the premicellar region suggests the appearance of new absorbing species as a result of electrostatic interaction of the dyes with anionic surfactant molecules in the premicellar region [8].

Petra Forte-Tavcer used spectrophotometry to investigate ion-pair complex formation between anionic dyes and cationic surfactants. Schaeppi Treadwell's and Schwarzenbach's methods were used for calculating the equilibrium constants of interactions. With both methods the equilibrium constants were determined at different



temperatures from the equimolar job's plots, which were also used to establish the composition of the associates.  $K$  values calculated at different temperatures show a decreasing tendency with increasing temperatures.  $\Delta G$ ,  $\Delta S$ ,  $\Delta H$  were also calculated [12]. The specific conductance of dye-surfactant mixtures was measured at 25, 35 and 45 °C by Sibel Tunc, and Osman Duman. A decrease in measured specific conductance values of dye-surfactant mixture was caused by the formation of non-conducting or less-conducting dye-surfactant complex. The equilibrium constants,  $K_1$ , the standard free energy changes,  $\Delta G_1^\circ$ , the standard enthalpy changes,  $\Delta H_1^\circ$  and the standard entropy changes,  $\Delta S_1^\circ$  for the first association step of dye-surfactant complex formation were calculated by a theoretical model. The increasing of temperature caused a decrease in the  $K$  and the negative  $\Delta G_1^\circ$  values for all the systems studied [28].

Sabina Bracko and Joze Span studied the formation of a dye-surfactant ion pair using a conductometric method in which the conductance of aqueous solutions of an anionic dye was measured in the presence of the cationic surfactants at four different temperatures. Two theoretical models to calculate the relevant equilibrium constants were derived. Both methods of calculation led to similar results that were in good agreement with other methods of investigation of dye-surfactant association. The results have shown that an increase in temperature lowers the tendency for ion pair formation as the equilibrium constants decrease with increasing temperature [29].

A. Navarro and F.Sanz studied the Complexation of an anionic dye with a series of nonionic surfactants with varying number of ethylene oxide units by voltammetry. From the measurement of the cathodic current of both dye and surfactant, the stability constants

of the established equilibrium between the dye  $D$ , the surfactant  $S$ , and the dye-surfactant complex  $D-S$  can be calculated [31].

Lai, C.C. and Chen, K.M. studied the dispersing abilities of a series of some surfactants toward some commercial dyes at elevated temperature, and the corresponding effects during polyester dyeing. From measurements of the dispersibilities and particle sizes of the dye solutions, they found that the surfactants exhibited good dispersing ability. Spectrophotometric methods confirmed that dye-surfactant complexes had formed. During the dyeing of polyester fabrics, the dyeing rate decreased when the surfactants were present because the hydrophilic dye-surfactant complexes enhanced the solubility of the disperse dyes [32].

Ahmadi, F., Daneshmehr, M.A. and Rahimi, M studied the effects of ionic surfactants (cationic and anionic) on dissociation constants and transition intervals of methyl red, methyl orange and cresol red. All studied dyes strongly interacted with cationic micelles [33].

Tehrani Bagha, A.R. , Bahrami, H. , Movassagh, B., Arami, M. and Menger, F.M. investigated the interactions of anionic azo dyes with a series of gemini cationic surfactants and dodecyl trimethyl ammonium bromide (DTAB) in aqueous solution have been investigated by means of UV-VIS spectroscopy. It was observed that the aggregation of surfactant and dye takes place at surfactant concentrations far below the critical micelle concentration of the individual surfactants. Aggregations with anionic dyes were reflected by hypsochromic shifts with a decrease in the intensity of absorption band. Further addition of surfactant results in an absorption spectrum of the dye characteristic in the presence of cationic micelles. The results also show bathochromic

shifts for MO followed by sharp increase in intensity of the absorption bands at  $\lambda_{\text{max}}$  after the CMC points of these surfactants. Such a behavior is observed for CR solutions in higher surfactant concentrations. The inhibiting effect of cationic surfactants on dye ability of cotton fabric with CR has also been studied at three different temperatures (30, 50, 90, 92 °C). Results show large differences between DTAB and Gemini cationic surfactants [34].

Moater, E.I., Olteanu, M., Ionita, I. and Ra dulescu, C. studied the interaction between nonionic surfactants and acid dyes. The formation of the complexes was determined by the surface tension method and by the UV-VIS spectrophotometry. The formation of some surfactant- dye complexes was made evident in the different molecular ratios in the submicellar zone compared to the micellar zone of concentration of the surfactant. There are different equilibria in the system which compete one another over a large scale of surfactant concentration (adsorption, micellisation, small complex formation, large complex -mixed micelles formation) [35].

Kartal, C. and Akbas, H. studied the interaction between an anionic dye and different surfactants, (anionic surfactant and nonionic surfactants) spectrophotometrically in a certain micellar concentration range. Light absorbances in the visible spectral range are measured as a function of mole fraction of surfactant at four different temperatures and at 24 h over the periodic time intervals. It is evident from the experimental measurements that nonionic surfactants form a complex with the anionic dye in aqueous solution in studied concentration range, while anionic surfactant does not [36].

Gokturk, S. studied the effect of hydrophobicity on micellar binding of an anionic dye, with various cationic surfactants spectrophotometrically in submicellar and micellar

concentration range. Going from aqueous solution to the more hydrophobic micellar environment the maximum absorbance of the anionic dye shifted to a higher wavelength. The binding constant ( $K_c$ ) values of the dye to cationic micelles were calculated by means of Benesi-Hildebrand Equation [37].

Yang, J. studied the interaction of aminoindophenol dye and ionic (cationic, anionic), zwitterionic and nonionic surfactants by their spectroscopic and surface properties. Large bathochromic shift (15 nm) in the absorption spectrum was found for aminoindophenol dye at high pH in cationic surfactant, while there is no significant shift in anionic, zwitterionic and nonionic surfactant solutions. Interaction of dye and surfactants on surface and in solution is correlated to the intensity of dye deposition on fiber. The charge complex formation between cationic surfactant and aminoindophenolic dye delays the dye diffusion into keratin fiber. The stronger is the dye/surfactant interaction, the lower dye deposition and diffusion becomes [38].

Oakes, J., Gratton, P., and Dixon, S. has made a spectroscopic study (UV-VIS and adsorption) of the interactions of select model azo dyes with a range of surfactant types and their mixtures both above and below their respective critical micelle concentrations. All surfactants inhibit adsorption of the dyes to cotton above their critical micelle concentrations due to incorporation in micelles. However, formation of 1:1 complexes between dyes and cationic or zwitterionic surfactants in sub-micellar regions results in enhanced deposition on cotton. It is shown that attractive or repulsive electrostatic interactions play a key role in dye binding to micelles. Unusually, spectra of complexes formed between the dye and cationic surfactant are typical of those of the azo tautomeric form as opposed to the hydrazone form that is prevalent in aqueous media. Addition of

anionic surfactant to micellar solutions of nonionic or zwitterionic surfactants results in successive displacement of dye from the respective micelles, i.e. binding is competitive [39].

## Chapter III

### Experimental

All experiments were carried out with analytical reagent grade chemicals using doubly distilled and deionized water.

#### 3.1.1 Chemicals

The names of chemicals used are listed in Table 3.1.

**Table 3.1**

**Data Including Chemicals with Abbreviations, Molecular Weight and Supplier**

Chemicals	Abbreviations	M.wt	Suppliers
<b><u>Dyes</u></b>			
Alizarin red S	ARS	342.26	Fluka
<b><u>Surfactants</u></b>			
Cetyltrimethylammonium bromide	CTAB	364.5	Biomedical

#### 3.1.2 Solution Preparation

The composition of the complex was determined from the equimolar mother solutions, while the equilibrium complexation constants were determined from the nonequimolar mother solutions of the dye and surfactant. The solutions were prepared according to Job's Method according to which both the equimolar and nonequimolar mother solutions were mixed in varying volume ratios but in such a way that the total volume of each mixture remained the same (10mL):X volume units of the surfactant solution were added

to (1-X) volume units of the dye solution. In this way a series of mixed solutions having various amounts ARS and CTAB were prepared.

#### **3.1.2.1 Solution preparation for the determination of the composition of the complex**

The stock solutions of both ARS and CTAB were prepared in deionized water. The mother solutions of the dye and surfactant with concentrations  $C_D^\circ$  and  $C_S^\circ$  respectively were prepared. Solutions were prepared in the concentration range in which it obeys Beer's Lambert law. For an equimolar mother solutions of the anionic dye and cationic surfactant in water,  $C_D^\circ = C_S^\circ = 2 \times 10^{-4}$  and  $1 \times 10^{-4} \text{ mol.dm}^{-3}$

The composition of the complex formed was determined from the equimolar mother solutions of the dye and surfactant.

#### **3.1.2.2 Solutions for the determination of the equilibrium complex formation constant at 25°C**

For nonequimolar mother solutions of the anionic dye and cationic surfactant in water,  $C_D^\circ = 3 \times 10^{-5}$ ,  $6 \times 10^{-5}$ , and  $8 \times 10^{-5} \text{ mol.dm}^{-3}$  and  $C_S^\circ = 3 \times 10^{-4} \text{ mol.dm}^{-3}$

#### **3.1.2.3 Solutions for the determination of the equilibrium complex formation constant at different temperatures**

For the determination of equilibrium complexation constants at different temperatures the nonequimolar mother solutions of the dye and surfactants were prepared as:

$C_D^\circ = 8 \times 10^{-5} \text{ mol.dm}^{-3}$  and  $C_S^\circ = 4 \times 10^{-4} \text{ mol.dm}^{-3}$

## **3.2 Ultraviolet Visible Spectroscopy**

### **3.2.1 Double-Beam Spectrophotometer**

Spectrophotometric measurements were performed on a Perkin-Elmer double-beam ultraviolet-visible spectrophotometer (Lambda-20) with 1.0 cm quartz cells. The instrument has two light paths, one for sample and other for the blank or reference. The detector alternately sees the reference and the sample beam and the output of the detector is proportional to the ratio of the intensities of the two beams  $I/I_0$ .

### **3.2.2 Measurement of Simple Absorption Spectra**

The visible absorption spectra of additive solutions containing surfactant in the concentration range, from premicellar concentration to postmicellar concentration, were recorded by using the spectrophotometer. Also the absorption spectra of the series of mixed solutions prepared according to Job's Method were recorded.



#### 4.1 Spectrophotometric Study of ARS-CTAB Complex Using Job's Method

The interactions between an amphiphilic anthraquinoid dye Alizarin Red S with a cationic surfactant cetyltrimethylammonium bromide in aqueous medium has been studied spectrophotometrically in the premicellar region using the method of continuous variations also called Job's Method. Molecular complexes having specific and characteristics physicochemical features are formed at concentrations below the CMC. Both electrostatic and hydrophobic interactions are involved in such type of complexations.

Job's Method has been widely used for the determination of coordination complexes in aqueous media, but its application to the study of dye-surfactant complexes or ion-pair associations has also been proved by most published data [2, 6, 12].

Our present work is related with the spectrophotometric determination of ion-pair association or complexation between ARS and a CTAB cationic surfactant in the premicellar region using Job's Method. Job's Method is capable of yielding both the stoichiometric composition and the association constant of the complex where a measured experimental property is a linear function of the concentration and where only one complex is important.

Spectrophotometric measurements are very suitable for applications of Job's Method, because light absorption is proportional to the concentration of the absorbing species, which is one of the necessary conditions for quantification.

#### 4.1.1 Equations Used For The Determination Of Different Parameters Of The Complex

**Job's Method** is used for the determination of Stoichiometric composition and equilibrium complex formation constant of the complex so formed in the premicellar region. According to Job's Method the mother solutions are mixed in varying volume ratios but in such a way that the total volume of each mixture remains the same: X volume units of the surfactant solution are added to (1-X) volume units of the dye solution.

$$X = \frac{V_s}{V_s + V_D} \quad (1)$$

'X' is the volume fraction of the surfactant,  $V_s$  is the volume taken from surfactant mother solution and  $V_D$  is the volume taken from the dye mother solution for the preparation of different volume fractions. In this way a series of mixed solutions having various amounts of the dye and surfactant are prepared and the absorbance of each solution is measured. A plot is made between the corrected absorbance ' $\Delta A$ ' of particular mixtures and the volume fraction of the surfactant 'X'. The maximum or minimum occurs at volume ratio  $X=X_m$ , corresponding to the combining ratio of dye and surfactant in the complex. " $X_m$ " is the volume fraction at which maximum absorbance is shown by the complex. The volume fraction corresponding to the maxima or minima of the plot of  $\Delta A$  Vs. X is the mixture in which maximum complexation takes place. The corrected absorbance ' $\Delta A$ ' is calculated as;

$$\Delta A = A_{\text{exp}} - A_{\text{theor}} \quad (2)$$

Where  $A_{\text{exp}}$  is the absorbance of the complex at a particular wavelength at which complexation is studied i.e., the absorbance observed directly from the spectrum.

And  $A_{\text{theor}}$  is the absorbance of the complex if no reaction has occurred i.e.,

$$A_{\text{theor}} = \epsilon_D C_D^\circ (1-X) + \epsilon_S C_S^\circ X \quad (3)$$

Where  $\epsilon_D C_D^\circ$  and  $\epsilon_S C_S^\circ$  are simply the absorbance of dye and surfactant mother solutions respectively observed at the wavelength of complexation, and  $(1-X)$  and  $X$  are the volume fractions of the dye and surfactant respectively in each mixture. Since ARS mother solution shows absorbance in the visible region while CTAB remains transparent in the visible region in which the complex absorbs, so the equation of our interest is the one in which absorbance due to surfactant is omitted i.e.,

$$A_{\text{theor}} = \epsilon_D C_D^\circ (1-X)$$

So

$$\Delta A = A_{\text{exp}} - \epsilon_D C_D^\circ (1-X) \quad (4)$$

Equation (4) is used for the calculation of  $\Delta A$  or the corrected absorbance.

The formation of the dye-surfactant complex in the premicellar region can be expressed as an equilibrium constant, the equilibrium complex formation constant ( $K_{\text{eq}}$ ) which is derived from the law of mass action [2]. If we consider the interaction between the anionic dye [ $D^-$ ] and cationic surfactant [ $S^+$ ] in terms of the equilibrium, Then the process can be written as:



The equilibrium complex formation constant ( $k_{\text{eq}}$ ) can be calculated from nonequimolar Job's plots using the following equation:

$$K_{eq} = \frac{(p-1)(1-2X_m)}{C_D^0[(p-1)X_m-1]^2} \quad (5)$$

Where “p” is the ratio between the dye and surfactant concentration or  $C_s^0 = p C_D^0$

#### 4.1.2 Calculations Of Thermodynamic Parameters

The equilibrium complex formation constant ( $K_{eq}$ ) is calculated at five different temperatures. Thermodynamic parameters like  $\Delta G$ ,  $\Delta H$ , and  $\Delta S$  are calculated making use of  $K_{eq}$  obtained at different temperatures.  $\Delta G$  is calculated using the following equation:

$$\Delta G = -RT \ln K_{eq} \quad (6)$$

Where ‘R’ is the general gas constant, T is the temperature in Kelvin.

‘ $\Delta H$ ’ is calculated using Van’t Hoff equation, according to which  $\ln K_{eq}$  is plotted Vs.  $1/T$ .

$\Delta H$  is calculated from the slope of the plot according to the following equation.

$$\ln K_{eq} = \frac{-\Delta H}{RT} \quad (7)$$

Multiplying slope with general gas constant gives the value of enthalpy of the reaction.

Entropy ‘ $\Delta S$ ’ is calculated using the following equation:

$$\Delta S = \frac{\Delta H - \Delta G}{T} \quad (8)$$

Our experimental portion consists of two sections.

### Section I

Section I further comprises of two parts:

**4.1.3 Part I:** is concerned with the selection of optimal parameters to be studied i.e.,

4.1.3.1 Concentration range of the dye

4.1.3.2 Wavelength of the dye to be studied and the concentration range of the surfactant to be used

4.1.3.3 Composition of the complex

4.1.3.4  $K_{eq}$  at room temperature

4.1.4 Part II: is concerned with;

4.1.4.1 Determination of  $K_{eq}$  at different Temperatures

4.1.4.2 Calculations of different thermodynamic parameters,  $\Delta G$ ,  $\Delta H$ , and  $\Delta S$

## Section II

4.2 IR spectroscopy and observation of FTIR spectra of ARS, CTAB and ARS-CTAB complex

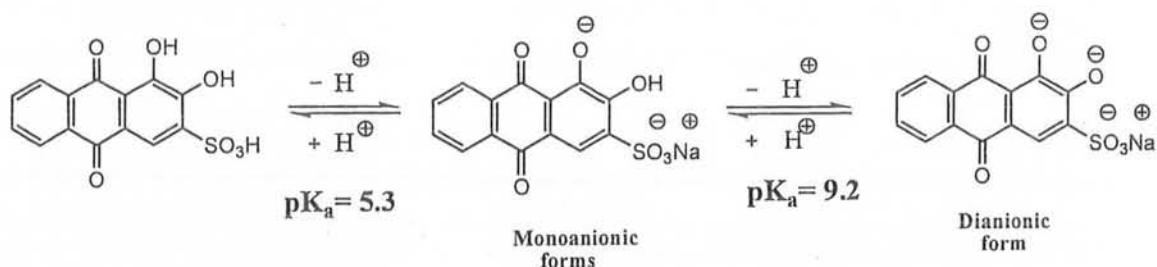
4.3 Suggesting the possible mechanism of interactions between ARS and CTAB in the premicellar region

## Section I

### 4.1.3 Part I

#### 4.1.3.1 Selection Of The Concentration Range Of The Dye

The amphiphilic anthraquinoid dye, Alizarin Red S (Mordant red 3), is used as organic additive. The molecular structures of Alizarin Red S used are shown as



Molecular structure of Alizarin Red S in aqueous medium

Alizarin Red S is a polyfunctional molecule with the  $\text{pK}_a$  values of 5.3 and 9.2.

Therefore, at  $\text{pH} < 5$ , ARS is an uncharged molecule, while at  $\text{pH} > 9$ , it is a dianion. In

the pH range from 5 to 9 a mixture of uncharged, monoanionic and dianionic forms of ARS exist. The position of the long wavelength absorption band of anthraquinoid dye is sensitive to medium effects.

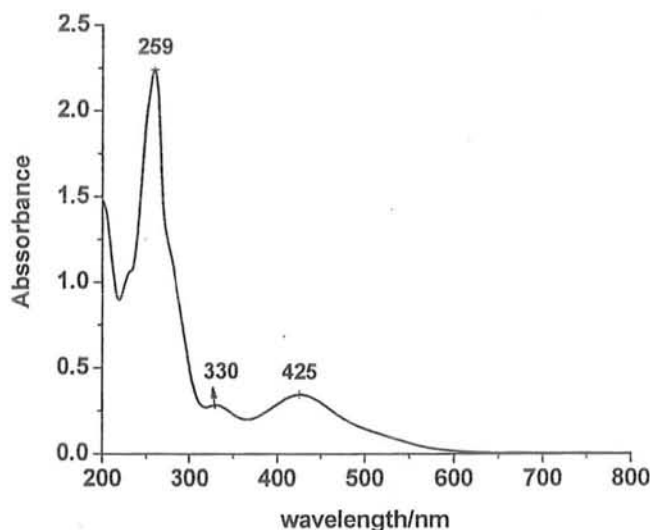


FIG. 4.1. UV-Visible spectra of Alizarin Red S in aqueous medium.

FIG.4.1. shows the absorption spectrum of ARS in aqueous medium. UV-spectra of ARS in aqueous medium exhibits two major absorption bands in the region 300-600nm. Both bands are the result of  $n-\pi^*$  transition owing to the presence of p-benzoquinone group, condensed between two rings in the structure of Alizarin Red S (ARS) dye giving absorption maximum at 330 and 426 nm respectively. The peak observed at 259 nm is attributed to benzene ring. While the other peak which stretches in the 340-440 nm region to give yellow colour to some of these compounds is due to p-benzoquinone group. The bathochromic shift is due to two hydroxyl groups (auxochrome) at the two substituted benzene ring. Change in absorption at maximum wavelength may results from structural strain and chromophore distortion. The selection criteria for choosing the concentration range was its behaviour under

the conditions of Beer Lambert law. One of the necessary conditions of the application of Job's Method is that the system should obey Beer's law [10]. That concentration range was taken as optimal range which observes the limitations set by Beer Lambert law. Different concentrations of ARS in aqueous medium were studied.

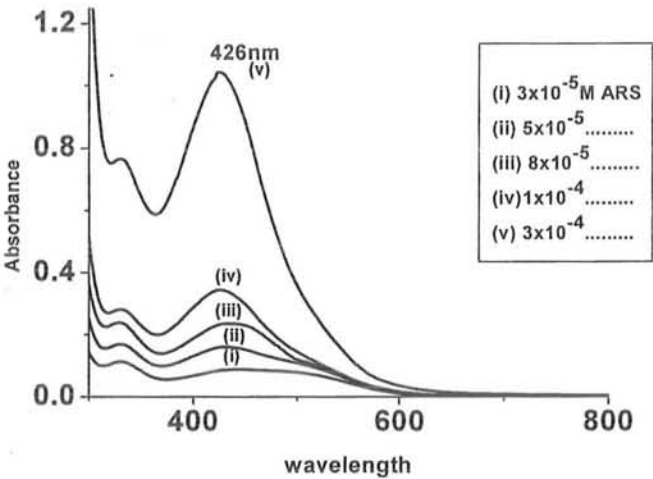


FIG.4.2. Plot of absorbance Vs. wavelength of different concentrations of ARS in aqueous medium

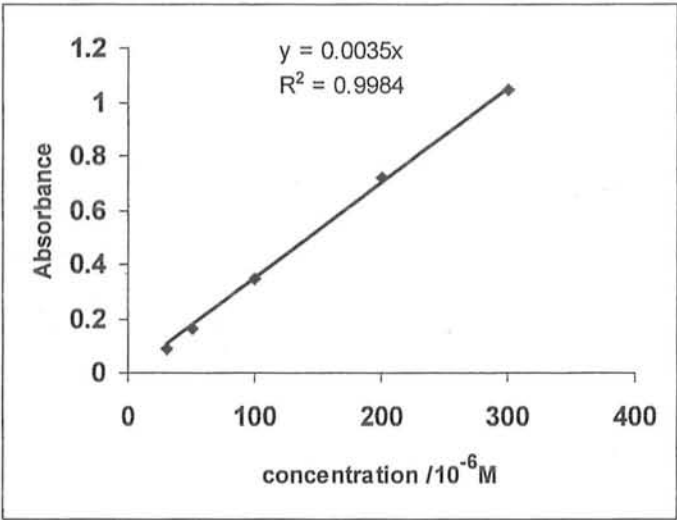


FIG.4.3. Plot of absorbance Vs. concentration of ARS in aqueous medium

FIG.4.2. shows the absorption spectra of different concentrations of ARS in aqueous medium. From the plot it is observed that absorption increases as the concentration of the dye increases. FIG.4.3 shows the plot of absorbance Vs. concentration of ARS in aqueous medium. The molar extinction coefficient of ARS calculated at 426 nm wavelength is  $3502.9 \text{ dm}^3 \cdot \text{mol}^{-1} \cdot \text{cm}^{-1}$ . The linearity of the plot indicates the validity of Beer's law in this concentration region; i.e., up to approximately  $3 \times 10^{-4} \text{ mol} \cdot \text{dm}^{-3}$  of the dye concentration can be used. As the concentration increases from  $3 \times 10^{-4} \text{ mol} \cdot \text{dm}^{-3}$  the absorbance exceeds '1'; i.e., deviation from Beer's law occurs. So the maximum limit up to which we can use the dye concentration is  $3 \times 10^{-4} \text{ mol} \cdot \text{dm}^{-3}$ .

#### **4.1.3.2 Selection Of The Concentration Range Of The Surfactant And wavelength Of the Dye To be Considered**

In order to select the wavelength of the dye with respect to which complexation is studied, and to determine the concentration range of the surfactant which is to be used, the effect of addition of the different concentrations of surfactant on the absorption spectra of Alizarin Red S is observed as:



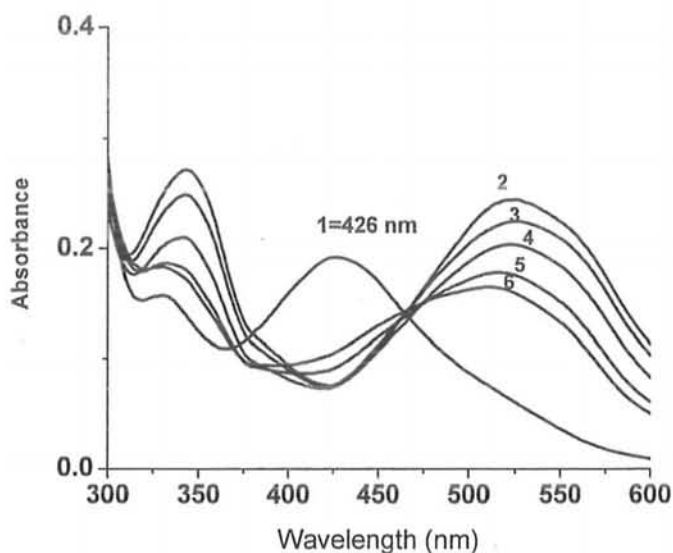


FIG.4.4. Visible absorption spectra of ARS ( $5 \times 10^{-5} \text{ mol.dm}^{-3}$ ) at various concentration of Cetyl trimethylammonium bromide (CTAB) at 298K. Concentration of CTAB: (1) 0.0; (2)  $1 \times 10^{-3} \text{ mol.dm}^{-3}$ ; (3)  $6.6 \times 10^{-4} \text{ mol.dm}^{-3}$ ; (4)  $3.33 \times 10^{-4} \text{ mol.dm}^{-3}$ ; (5)  $9.86 \times 10^{-5} \text{ mol.dm}^{-3}$ ; (6)  $6.5 \times 10^{-5} \text{ mol.dm}^{-3}$ .

FIG.4.4. shows the effect of different concentrations of CTAB on the absorption spectra of Alizarin Red S. The concentration of the dye is kept constant i.e.,  $5 \times 10^{-5} \text{ mol.dm}^{-3}$ . Curve "1" is the absorption spectra of the dye, while the region from 2-6 indicates the effect of decreasing concentration of surfactant from post micellar to premicellar region. With the addition of CTAB a bathochromic shift from 426-526 nm takes place as shown in figure 4.4. An isobestic point is observed at about 462 nm. Even the addition of small concentration of surfactant causes a high bathochromic shift. It is more clear from table. 4.1, figures. 4.5 and 4.6. which are mathematical representations of figure.4.4.

**Table 4.1 Absorbance and maximum wavelength of ARS in aqueous solutions of CTAB**

( $C_s$ =concentrations of CTAB) taking  $\lambda_{\max}$ =426 nm of ARS into considerations

$C_s$ (mol dm <sup>-3</sup> )	Absorbance	$\lambda_{\max}(\text{nm})$
0	0.192	426
$6.50 \times 10^{-5}$	0.165	509
$9.86 \times 10^{-5}$	0.178	514
$1.48 \times 10^{-4}$	0.188	518
$2.22 \times 10^{-4}$	0.196	522
$3.33 \times 10^{-4}$	0.204	522
$5.00 \times 10^{-4}$	0.217	524
$6.66 \times 10^{-4}$	0.225	525
$1.00 \times 10^{-3}$	0.244	525
$1.33 \times 10^{-3}$	0.246	526

Table.4.1. shows the Absorbance and  $\lambda_{\max}$  values observed from FIG.4.4. As concentration of the surfactant increases, the absorbance values increase. The increase in absorbance is abrupt in the premicellar region while in the micellar region the change in absorbance is very small. This behaviour is shown graphically for the sake of convenience in FIG 4.5. Similar is the case with the wavelength of maximum absorbance. We see that at the lower surfactant concentration the wavelength keeps on showing a changing behaviour while after a certain concentration a constancy is observed in the wavelength of maximum absorbance. This behavior is more clearly shown in FIG.4.6.

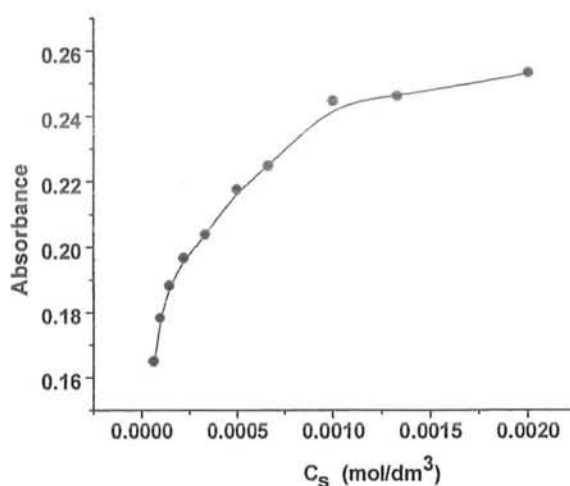


FIG.4.5. Plot of Absorbance Vs.concentration of the complex from premicellar to Postmicellar concentrations of the CTAB

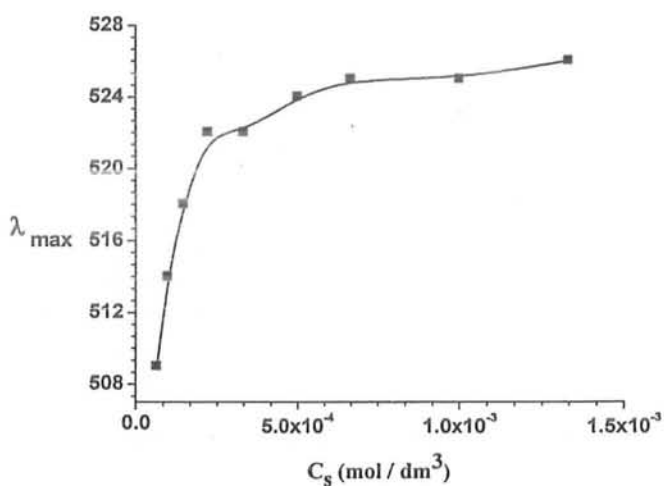


FIG.4.6. Plot of  $\lambda_{\text{max}}$  Vs.concentration of the complex from premicellar to Postmicellar concentrations of the CTAB

The region in which both the absorbance and wavelength of maximum absorbance becomes constant is the micellar region. The micellar system is a more stable system, in which surfactant molecules are in the form of aggregates and thus entraps the dye monomer. While the abrupt change observed in absorbance and wavelength of maximum

absorbance in the premicellar region needs some explanation. Most of the scientists have attempted to explain the observed behaviour in the premicellar region. Spectral changes are observed when oppositely charged surfactants and dyes are interacted in the premicellar region. These spectral changes are attributed to the formation of different chemical species [3, 8]. To explain these different chemical species formed at the low surfactant concentrations various methods have been used. One such method is Job's Method, which is capable of yielding both the composition of the complex and equilibrium complex formation constant of the complexes so formed in the premicellar region. An isobestic point is observed in FIG.4.4. at about 462 nm. The appearance of isobestic point is the indication of 1:1 complex formation [2]. So our simple absorption spectra is also in the favour of 1:1 complexation between ARS and CTAB in the premicellar region. Next we have attempted to confirm the composition of the complex by applying Job's Method.

#### **4.1.3.3 Determination Of The Composition Of The Complex**

In order to determine the composition of the complex equimolar mother solutions of both dye and surfactant are used. The term "mother solution" means the stock solution.  $C_s^0$  and  $C_D^0$  are the concentrations of surfactant and dye mother solutions respectively. Both the equimolar mother solutions are mixed in varying volume ratios but in such a way that the total volume of each mixture remained the same. The volume was kept constant up to 10 mL. A series of mixed solutions having various amounts of ARS and CTAB was prepared starting from '0' volume fraction of the CTAB to '1' volume fraction of CTAB. "0" volume fraction of CTAB means the solution in which '0' mL of CTAB and '10' mL of ARS is present i.e., solution containing ARS only. Similarly '1' volume

fraction of CTAB means the solution containing CTAB only. The region between '0' and '1' volume fractions of the series indicate mixtures consisting of ARS and CTAB in different volume ratio. The absorbance of each solution was measured [2]. Since maximum shift is observed at the 426 nm, so complexation was studied in the range 400-600 nm. The shift which occurs with respect to wavelength of maximum absorbance of the dye, is noted. The shift in  $\lambda_{\max}$  is actually the indication of complex formation between ARS and CTAB, because the surfactant is transparent in the visible region and ARS has its characteristic peak in the region up to 440 nm. So the newly appeared peak above 500 nm cannot be assigned either to ARS or CTAB. In order to study the complexation phenomenon one wavelength is taken into account for calculation purposes. Volume fractions are calculated using equation (1) and  $\Delta A$  is calculated using equation (4). The maximum of the plot between  $\Delta A$  and X (volume fraction of surfactant) indicates the mixture in which maximum amount of the complex is present or in which stoichiometric amount of ARS and CTAB are present. The composition of the complex is determined by using equimolar stock solutions of ARS and CTAB. The composition of the complex is determined by using

**4.1.3.3.1** CTAB and ARS stock solutions of concentration  $C_s^0 = C_D^0 = 2 \times 10^{-4} \text{M}$

**4.1.3.3.2** CTAB and ARS stock solutions of concentrations  $C_s^0 = C_D^0 = 1 \times 10^{-4} \text{M}$

#### 4.1.3.3.1 Determination Of the Composition Of Complex when

$$C_s^0 = C_D^0 = 2 \times 10^{-4} \text{ mol.dm}^{-3}$$

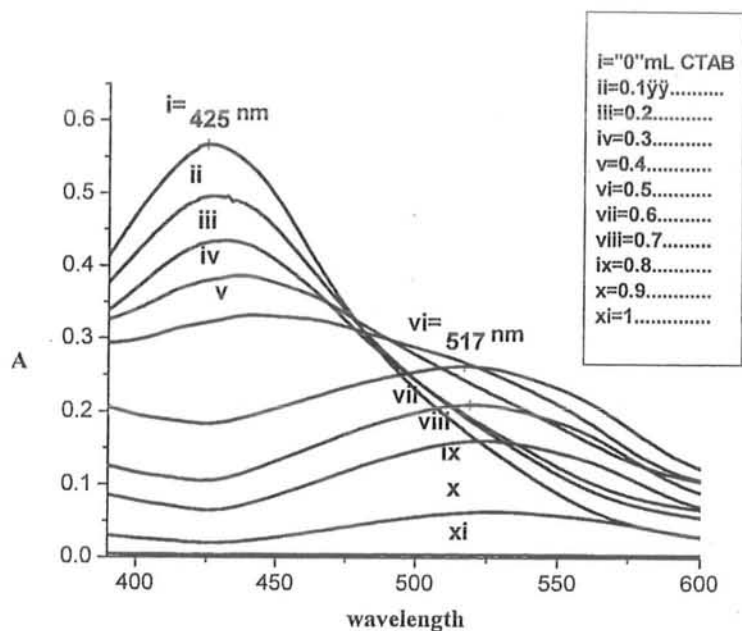


FIG.4.7. Plot of Absorbance Vs wavelength of different volume fractions of the complex made from equimolar mother solutions of ARS and CTAB( $C_s^0 = C_D^0 = 2 \times 10^{-4} \text{ mol.dm}^{-3}$ )

FIG.4.7. shows the UV-spectra of a series of mixtures consisting of different amounts of both dye and surfactant. "i" and "xi" are the absorption spectra of the dye and surfactant respectively in visible region 400-600. The wavelength of maximum absorbance of the dye occurs at 425 nm while surfactant shows no absorbance in the mentioned wavelength range. The region between "i" and "xi" shows the absorption spectra of the different fractions prepared by mixing the equimolar mother solutions of both dye and surfactant in various volume ratios. The wavelength of maximum absorbance changes from 425 nm for the dye alone to about 517 nm for the complex. A slight shift above or below from

517 nm may occur, but for calculation purposes one wavelength should be taken into account. Of the series of solutions prepared so far one mixture is such which contains the complex in maximum amount. This can be observed from spectral measurements for absorbance i.e., corrected absorbance ( $\Delta A$ ), which is calculated using equation (4). Table.4.2. shows calculations for the exact absorbance or the corrected absorbance ( $\Delta A$ ). Volume fraction with respect to CTAB is calculated using equation (1).

**Table.4.2. Calculations for the corrected absorbance of the complex formed as a result of interactions between ARS & CTAB ( $C_s = C_D = 2 \times 10^{-4} \text{ mol} \cdot \text{dm}^{-3}$ )**

$\Delta A = A_{\text{exp}} - \epsilon_D C_D^0 (1-X)$ $\epsilon_D C_D^0 = A_{\text{dye}} = 0.17564 \text{ at } 517\text{nm}$			
X	$A_{\text{exp}}$	$A_{\text{theor}}$	$\Delta A$
0	0	0	0
0.1	0.194	0.158	0.036
0.2	0.198	0.141	0.057
0.3	0.244	0.123	0.121
0.4	0.268	0.105	0.163
0.5	0.263	0.088	0.175
0.6	0.210	0.070	0.140
0.7	0.160	0.053	0.107
0.8	0.119	0.035	0.084
0.9	0.062	0.017	0.045
1	0	0	0

Table.4.2.shows calculations of the corrected absorbance ( $\Delta A$ ) for the complex at 517 nm.

The values of " $\Delta A$ " calculated so far are given in Table .4.2. A plot of " $\Delta A$ " Vs. " $X$ " is shown in FIG.4.8.

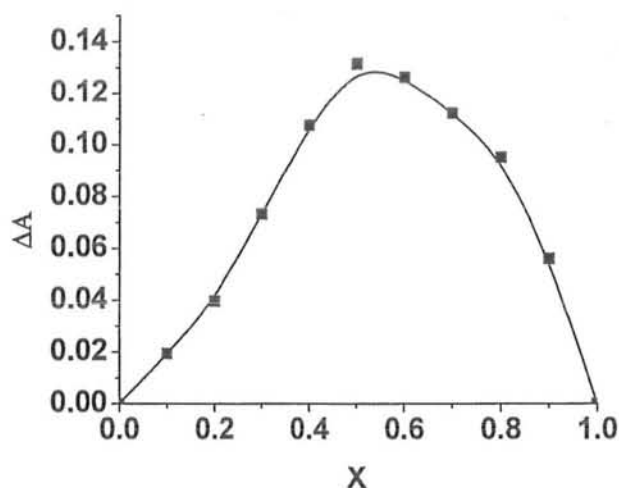


FIG.4.8. Job's plot ( $\Delta A$  Vs. volume fraction of surfactant solutions,  $X$ ) for equimolar mother solutions of ARS and CTAB in water at 298K.  $C_s^0 = C_D^0 = 2 \times 10^{-4} \text{ mol.dm}^{-3}$

From FIG.4.8. it is observed that absorbance of the complex increases up to a certain fraction and then decreases. The volume fraction at which the maximum absorbance occurs is the fraction in which ARS and CTAB are in the stoichiometric ratio. In the present case it occurs at 0.5, which indicates the 1:1 stoichiometric ratio of the dye and surfactant. It means that maximum complexation occurs when both dye and surfactant are present equal amounts. To see whether changing the concentrations of equimolar mother solutions of the dye and surfactant has any change on the stoichiometry of the complex formed, the above procedure was repeated for  $1 \times 10^{-4} \text{ M}$  solutions of both of the dye and surfactant solutions.



4.1.3.3.2 Determination Of the Composition Of Complex when

$C_s^0 = C_D^0 = 1 \times 10^{-4} \text{ mol.dm}^{-3}$

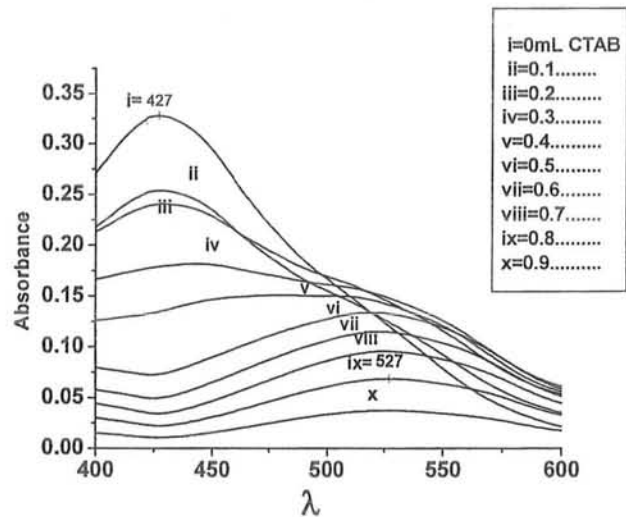


FIG.4.9. Plot of Absorbance Vs. wavelength of different volume fractions of the complex made from equimolar mother solutions of ARS and CTAB ( $C_s^0 = C_D^0 = 1 \times 10^{-4} \text{ mol.dm}^{-3}$ )

FIG.4.9. shows the UV-spectra of a series of mixtures consisting of different amounts of both dye and surfactant. "i" is the absorption spectra of the dye in visible region 400-600nm. The wavelength of maximum absorbance of the dye occurs at 427 nm in this case while surfactant shows no absorbance in the mentioned wavelength range. The region from "ii" and "x" shows the absorption spectra of the different fractions volume fractions of CTAB. The wavelength of maximum absorbance changes from 427 nm for the dye alone to about 527 nm for the complex. In order to find out the mixture in which maximum complexation has occurred the corrected absorbance ( $\Delta A$ ) is calculated using the same equation (4). Table.4.3. shows calculations for the exact absorbance or the corrected absorbance ( $\Delta A$ ).

Table.4.3. Calculations for the corrected absorbance of the complex formed as a result of interactions b/w ARS & CTAB ( $C_s = C_D = 1 \times 10^{-4} \text{ mol. dm}^{-3}$ )

$\Delta A = A_{\text{exp}} - \epsilon_D C_D^0 (1-X)$ $\epsilon_D C_D^0 = A_{\text{dye}} = 0.12177 \text{ at } 527 \text{ nm}$			
X	$A_{\text{exp}}$	$A_{\text{theor}}$	$\Delta A$
0	0	0	0
0.1	0.125	0.110	0.015
0.2	0.145	0.097	0.048
0.3	0.148	0.085	0.063
0.4	0.142	0.073	0.069
0.5	0.133	0.061	0.072
0.6	0.114	0.049	0.065
0.7	0.095	0.036	0.059
0.8	0.068	0.024	0.044
0.9	0.037	0.012	0.025
1	0	0	0

Table.4.3.shows calculations of the corrected absorbance ( $\Delta A$ ) for the complex at 527nm.

The values of " $\Delta A$ " calculated so far are given in Table .4.3. A plot of " $\Delta A$ " Vs. "X" is shown in FIG.4.10.

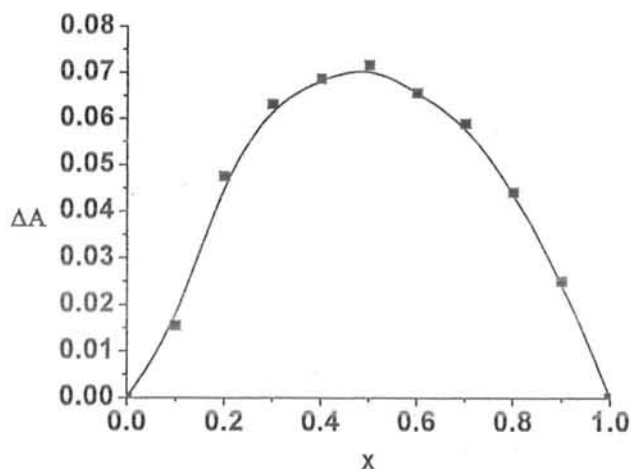


FIG.4.10. Job's plot ( $\Delta A$  Vs. volume fraction of surfactant solutions,  $X$ ) for equimolar mother solutions of ARS and CTAB in water at 298K.  $C_s^0 = C_D^0 = 1 \times 10^{-4} \text{ mol.dm}^{-3}$

FIG.4.10. shows that same trend is observed as in section 4.1.3.3.1 i.e., absorbance of the complex increases up 0.5 and then decreases. It means that the complex has 1:1 stoichiometric ratio of the dye and surfactant. Thus it can be concluded that the changing concentrations of the equimolar mother solutions of ARS and CTAB has no influence on the stoichiometry of the complex formed by their interaction. For the sake of convenience the combined plot is shown as

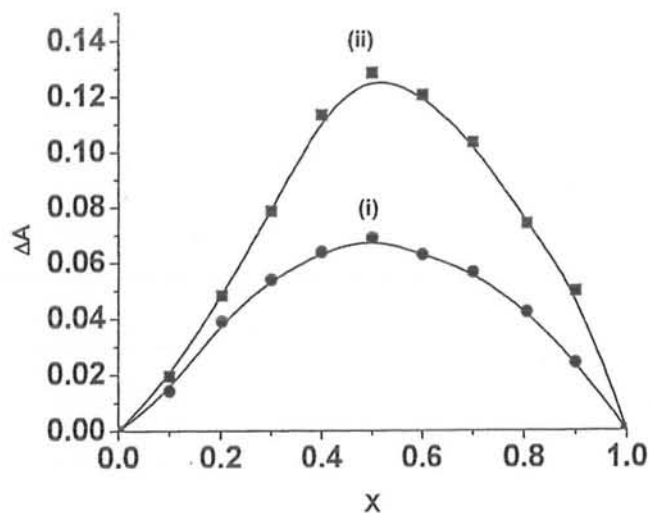


FIG.4.11. Job's plot ( $\Delta A$  vs. volume fraction of surfactant solutions,  $X$ ) for equimolar mother solutions of ARS and CTAB in water at 298K.  $C_s^0 = C_D^0$ ; (i)  $1 \times 10^{-4} \text{ mol.dm}^{-3}$  (ii)  $2 \times 10^{-4} \text{ mol.dm}^{-3}$

Next we have determined the equilibrium complex formation constant by interacting nonequimolar stock solutions of ARS and CTAB at room temperature, and observed the effect of changing concentration of the dye on the equilibrium composition constant.

#### 4.1.3.4 Determination of equilibrium Complex formation Constant at Room Temperature

If we consider the interaction between the anionic dye  $[D^-]$  and cationic surfactant  $[S^+]$  in terms of the equilibrium, then the process can be written as



The equilibrium complex formation constant ( $k_{eq}$ ) can be calculated from nonequimolar Job's plots using equation (5).

Equilibrium complex formation constant was determined by interacting three different concentrations of dye mother solutions with the surfactant solution of the same mother concentration, i.e.,  $C_S^\circ = 3 \times 10^{-4} \text{ mol.dm}^{-3}$ ,  $C_D^\circ = 3 \times 10^{-5}$ ,  $6 \times 10^{-5}$  and  $8 \times 10^{-5} \text{ mol.dm}^{-3}$ .

Series of solution is prepared in the same manner as discussed in section 4.1.3.3 for the determination of the composition of the complex. Volume fractions (X) and Corrected absorbance  $\Delta A$  and are calculated in the same way as done in section 4.1.3.3 using equations (1) and (4) respectively.

#### 4.1.3.4.1 Determination Of Equilibrium Complex Formation Constant When

$C_S^\circ = 3 \times 10^{-4} \text{ mol.dm}^{-3}$  and  $C_D^\circ = 3 \times 10^{-5} \text{ mol.dm}^{-3}$

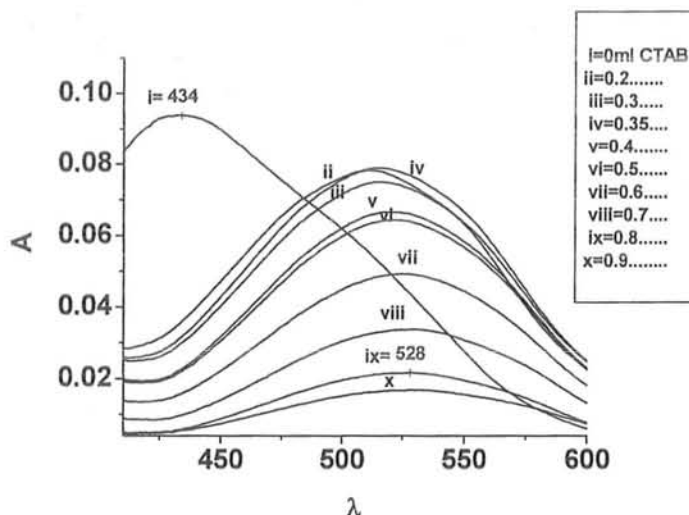


FIG.4.12. Plot of absorbance Vs. wavelength of different volume fractions of the complex using nonequimolar mother solutions of ARS and CTAB ( $C_S^\circ = 3 \times 10^{-4} \text{ mol.dm}^{-3}$ ,  $C_D^\circ = 3 \times 10^{-5} \text{ mol.dm}^{-3}$ )

FIG.4.12. shows the UV-spectra of a series of mixtures consisting of different amounts of both dye and surfactant. "i" is the absorption spectra of the dye. The wavelength of maximum absorbance of the dye occurs at 434 nm in this case. The region from "ii" and "x" shows the absorption spectra of the different fractions prepared by mixing the nonequimolar mother solutions of both dye and surfactant in various volume ratios. The wavelength of maximum absorbance changes from 434 nm for the dye alone to about 528 nm for the complex. Although a wide range of volume fractions differing in small increments were made, but in the spectra the absorption of the volume fractions of our particular concern are shown. Table.4.4. shows calculations for the exact absorbance or the corrected absorbance ( $\Delta A$ ).

Table.4.4. Calculations for the corrected absorbance of the complex formed as a result of interactions b/w ARS & CTAB ( $C_s^* = 3 \times 10^{-4}$  mol. dm<sup>-3</sup>,  $C_D^* = 3 \times 10^{-5}$  mol. dm<sup>-3</sup>)

$\Delta A = A_{\text{exp}} - \epsilon_D C_D^0 (1-X)$ $\epsilon_D C_D^0 = A_{\text{dye}} = 0.04368 \text{ at } 528 \text{ nm}$			
X	A <sub>exp</sub>	A <sub>theor</sub>	ΔA
0	0	0	0
0.2	0.074	0.035	0.039
0.25	0.081	0.033	0.048
0.3	0.073	0.031	0.042
0.35	0.077	0.028	0.049
0.4	0.066	0.026	0.040
0.5	0.064	0.022	0.042
0.6	0.049	0.017	0.032
0.7	0.034	0.013	0.021
0.8	0.022	0.009	0.013
0.9	0.017	0.004	0.013
1	0	0	0

Table.4.4.shows calculations of the corrected absorbance (ΔA) for the complex at 528 nm.

The values of “ΔA” calculated so far are given in Table .4.4. A plot of “ΔA” Vs. “X” is shown in FIG.4.13.

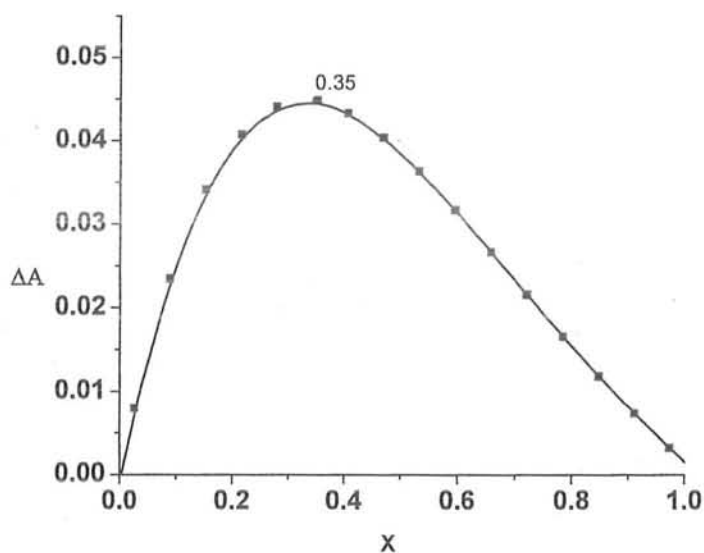


FIG.4.13. Job's plot ( $\Delta A$  vs. volume fraction of surfactant solutions,  $X$ ) for nonequimolar mother solutions of CTAB and ARS in water at 298 K.  $C_S^0 = 3 \times 10^{-4} \text{ mol} \cdot \text{dm}^{-3}$ ,  $C_D^0 = 3.0 \times 10^{-5} \text{ mol} \cdot \text{dm}^{-3}$

From FIG.4.13. it is observed that using the nonequimolar mother solution of the dye and surfactant the maximum absorbance occurs at 0.35 volume fraction of the surfactant solution in the present case. So,  $X_m = 0.35$ . Now putting the value of " $X_m$ " in equation (5) for the determination of equilibrium complex formation constant,  $K_{eq}$  is calculated as

Table.4.5. Calculations of  $K_{eq}$  when  $C_S^0 = 3 \times 10^{-4} \text{ mol} \cdot \text{dm}^{-3}$  and  $C_D^0 = 3 \times 10^{-5} \text{ mol} \cdot \text{dm}^{-3}$

$C_S^0 / \text{mol} \cdot \text{dm}^{-3}$	$C_D^0 / \text{mol} \cdot \text{dm}^{-3}$	$P = C_S^0 / C_D^0$	$X_m$	$1 - 2X_m$	$(p-1)(1-2X_m)$	$K_{eq} (\text{mol}^{-1} \cdot \text{dm}^3)$
$3 \times 10^{-4}$	$3 \times 10^{-5}$	10	0.35	0.3	2.70	$1.95 \times 10^4$

#### 4.1.3.4.2 Determination Of Equilibrium Complex Formation Constant When

$C_S = 3 \times 10^{-4} \text{ mol.dm}^{-3}$  and  $C_D = 6 \times 10^{-5} \text{ mol.dm}^{-3}$

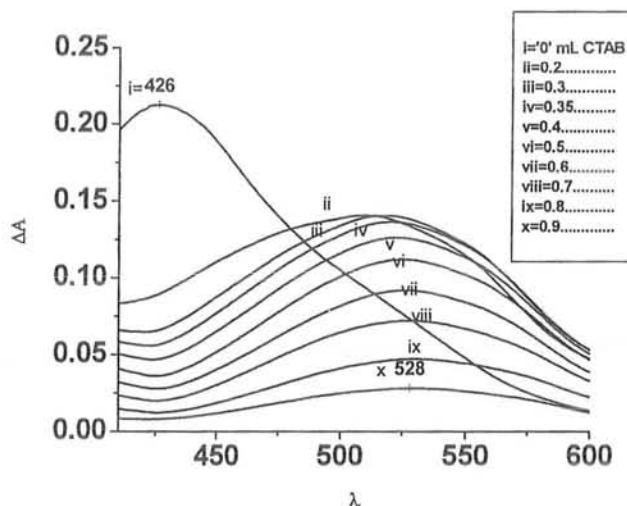


FIG.4.14. Plot of Absorbance Vs wavelength of different volume fractions of the complex made from nonequimolar mother solutions of ARS and CTAB ( $C_S = 3 \times 10^{-4} \text{ mol.dm}^{-3}$ ,  $C_D = 6 \times 10^{-5} \text{ mol.dm}^{-3}$ )

FIG.4.14. shows the UV-spectra of a series of mixtures consisting of different amounts of both dye and surfactant. "i" is the absorption spectra of the dye. The wavelength of maximum absorbance of the dye occurs at 426 nm. The region from "ii" and "x" shows the absorption spectra of the different fractions prepared by mixing the nonequimolar mother solutions of both dye and surfactant in various volume ratios. The wavelength of maximum absorbance changes from 426 nm for the dye alone to about 528 nm for the complex. Table.4.6. shows calculations for the corrected absorbance ( $\Delta A$ ).



Table.4.6.Calculations for the corrected absorbance of the complex formed as a result of interactions b/w ARS & CTAB ( $C_s = 3 \times 10^{-4} \text{ mol. dm}^{-3}$ ,  $C_D = 6 \times 10^{-5} \text{ mol. dm}^{-3}$ )

$\Delta A = A_{\text{exp}} - \epsilon_D C_D^0 (1-X)$ $\epsilon_D C_D^0 = A_{\text{dye}} = 0.07325 \text{ at } 528 \text{ nm}$			
X	$A_{\text{exp}}$	$A_{\text{theor}}$	$\Delta A$
0	0	0	0
0.2	0.133	0.059	0.074
0.3	0.136	0.051	0.085
0.35	0.135	0.048	0.087
0.4	0.126	0.044	0.082
0.5	0.112	0.037	0.075
0.6	0.092	0.029	0.063
0.7	0.072	0.022	0.050
0.8	0.047	0.015	0.032
0.9	0.028	0.007	0.021
1	0	0	0

Table.4.6.shows calculations of the corrected absorbance ( $\Delta A$ ) for the complex at 528 nm.

The values of “ $\Delta A$ ” calculated so far are given in Table .4.6. A plot of “ $\Delta A$ ” Vs. “X” is shown in FIG.4.15

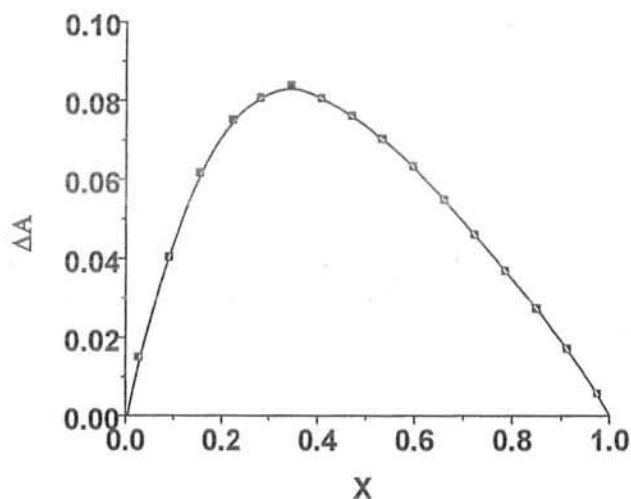


FIG.4.15. Job's plot ( $\Delta A$  vs. volume fraction of surfactant solutions,  $X$ ) for nonequimolar mother solutions of CTAB and ARS in water at 298 K.  $C_S^0 = 3 \times 10^{-4} \text{ mol} \cdot \text{dm}^{-3}$ ,  $C_D^0 = 6.0 \times 10^{-5} \text{ mol} \cdot \text{dm}^{-3}$

From FIG.4.15, it is observed that using the nonequimolar mother solution of the dye and surfactant the maximum absorbance occurs at 0.35 volume fraction of the surfactant solution in the present case. So,  $X_m = 0.35$ . Now putting the value of " $X_m$ " in equation (5) for the determination of equilibrium complex formation constant,  $K_{eq}$  is calculated as

Table.4.7. Calculations of  $K_{eq}$  when  $C_S^0 = 3 \times 10^{-4} \text{ mol} \cdot \text{dm}^{-3}$  and  $C_D^0 = 6 \times 10^{-5} \text{ mol} \cdot \text{dm}^{-3}$

$C_S^0 / \text{mol} \cdot \text{Dm}^{-3}$	$C_D^0 / \text{mol} \cdot \text{dm}^{-3}$	$P = C_S^0 / C_D^0$	$X_m$	$1-2X_m$	$(p-1)(1-2X_m)$	$K_{eq}(\text{mol}^{-1} \cdot \text{dm}^3)$
$3 \times 10^{-4}$	$6 \times 10^{-5}$	5.00	0.35	0.3	1.20	$1.25 \times 10^5$

#### 4.1.3.4.3 Determination Of Equilibrium Complex Formation Constant When

$C_S^\circ = 3 \times 10^{-4} \text{ mol.dm}^{-3}$  and  $C_D^\circ = 8 \times 10^{-5} \text{ mol.dm}^{-3}$

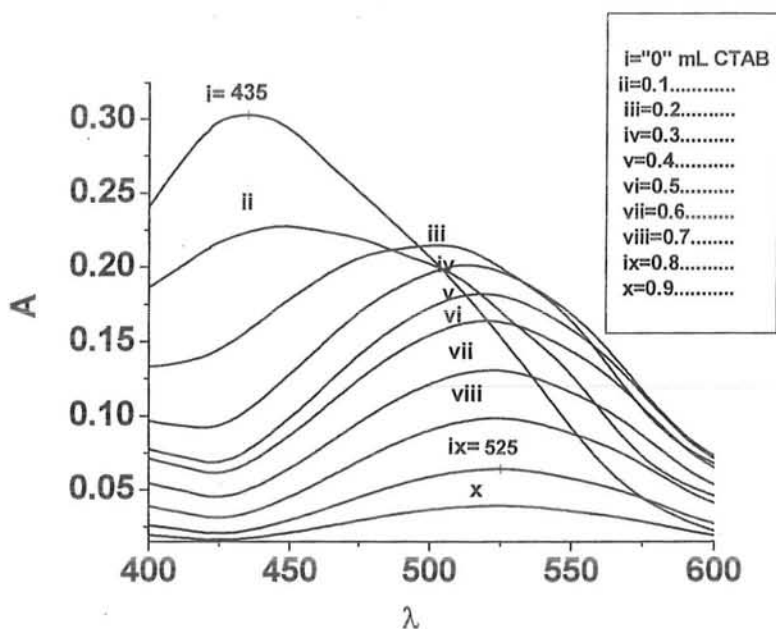


FIG.4.16. Plot of Absorbance VS wavelength of different volume fractions of the complex made from nonequimolar mother solutions of ARS and CTAB ( $C_S^\circ = 3 \times 10^{-4} \text{ mol.dm}^{-3}$ ,  $C_D^\circ = 8 \times 10^{-5} \text{ mol.dm}^{-3}$ )

FIG.4.16. shows the UV-spectra of a series of mixtures consisting of different amounts of both dye and surfactant. "i" is the absorption spectra of the dye. The wavelength of maximum absorbance of the dye occurs at 435 nm in this case. The region from "ii" and "x" shows the absorption spectra of the different fractions prepared by mixing the nonequimolar mother solutions of both dye and surfactant in various volume ratios. The

wavelength of maximum absorbance changes from 435 nm to about 525 nm for the complex. Table.4.8. shows calculations for the corrected absorbance ( $\Delta A$ ) at 525 nm .

Table.4.8. Calculations for the corrected absorbance of the complex formed as a result of interactions b/w ARS & CTAB ( $C_s^* = 3 \times 10^{-4} \text{ mol. dm}^{-3}$ ,  $C_D^* = 8 \times 10^{-5} \text{ mol. dm}^{-3}$ )

$\Delta A = A_{\text{exp}} - \epsilon_D C_D^0 (1-X)$ $\epsilon_D C_D^0 = A_{\text{dye}} = 0.16929 \text{ at } 525 \text{ nm}$			
X	$A_{\text{exp}}$	$A_{\text{theor}}$	$\Delta A$
0	0	0	0
0.1	0.182	0.152	0.030
0.2	0.208	0.135	0.073
0.3	0.201	0.119	0.082
0.4	0.182	0.102	0.080
0.5	0.164	0.085	0.079
0.6	0.131	0.068	0.063
0.7	0.098	0.051	0.047
0.8	0.064	0.034	0.030
0.9	0.039	0.017	0.022
1	0	0	0

Table.4.8.shows calculations of the corrected absorbance ( $\Delta A$ ) for the complex at 525 nm.

The values of " $\Delta A$ " calculated so far are given in Table .4.8. A plot of " $\Delta A$ " Vs. "X" is shown in FIG.4.17

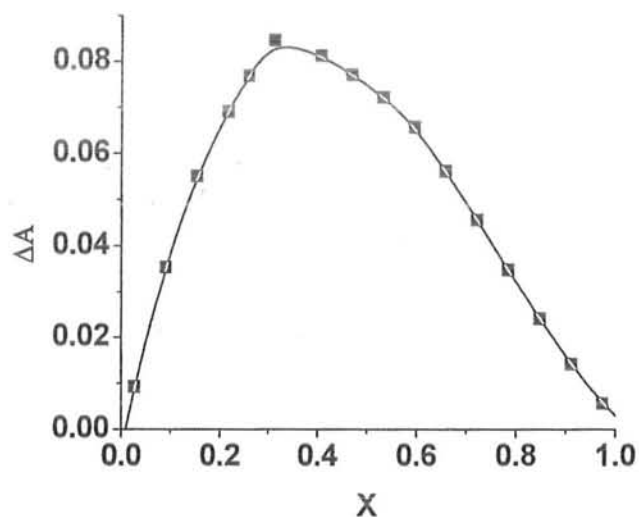


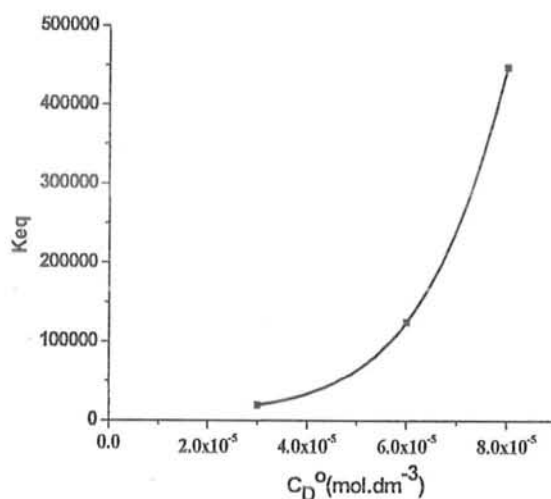
FIG.4.17. Job's plot ( $\Delta A$  vs. volume fraction of surfactant solutions,  $X$ ) for nonequimolar mother solutions of CTAB and ARS in water at 298 K.  $C_S^0 = 3 \times 10^{-4} \text{ mol} \cdot \text{dm}^{-3}$ ,  $C_D^0 = 8.0 \times 10^{-5} \text{ mol} \cdot \text{dm}^{-3}$

FIG.4.17. it is observed that maximum absorbance occurs at 0.3 volume fraction of the surfactant solution in the present case. So,  $X_m = 0.3$ . Using equation (5) equilibrium complex formation constant,  $K_{eq}$  is calculated as

Table.4.9. Calculations of  $K_{eq}$  when  $C_S^0 = 3 \times 10^{-4} \text{ mol} \cdot \text{dm}^{-3}$  and  $C_D^0 = 8 \times 10^{-5} \text{ mol} \cdot \text{dm}^{-3}$

$C_S^0 / \text{mol} \cdot \text{dm}^{-3}$	$C_D^0 / \text{mol} \cdot \text{dm}^{-3}$	$P = C_S^0 / C_D^0$	$X_m$	$1 - 2X_m$	$(p-1)(1-2X_m)$	$K_{eq} (\text{mol}^{-1} \cdot \text{dm}^3)$
$3 \times 10^{-4}$	$8 \times 10^{-5}$	3.75	0.3	0.4	1.10	$4.49 \times 10^5$

All the three results can be shown graphically as



**FIG.4.18. Plot of equilibrium complex formation constant ( $K_{eq}$ ) in water Vs. the mother solution concentrations of ARS at 298 K**

From Tables.4.5, 4.7 and 4.9 it is cleared that as the concentration of the dye increases the equilibrium complexation also increases. It can be explained as that at first the surfactant monomers are adsorbed at the interface with their hydrophobic part oriented outside of the bulk and their hydrophilic head group towards the aqueous medium. While dye molecules are present inside the bulk in such a way that their anionic head groups (sulphonate) are oriented towards the cationic head group (ammonium) of the surfactant. In this way a strong electrostatic interactions occur between these oppositely charged dye and surfactant. As the concentration of the dye increases while that of surfactant remains the same, in other words the number of molecules of the dye increases these interactions become even stronger. More dye molecules will be available to make complexes with the surfactant and thus results in high values of the equilibrium complex formation constant.

## 4.1.4 PART II

### 4.1.4.1 Determination of $K_{eq}$ at different Temperatures

To see whether temperature has any effect on the equilibrium complex formation constant, CTAB and ARS having concentration  $C_s^0 = 4 \times 10^{-4} \text{ mol.dm}^{-3}$  and  $C_D^0 = 8 \times 10^{-5} \text{ mol.dm}^{-3}$  respectively are interacted at five different temperatures i.e., 20, 25, 30, 35 and 40°C and  $K_{eq}$  is determined at the mentioned temperatures.

Same procedures are adapted for the determination of equilibrium complex formation constant at different temperatures as we have for the determination of the same parameter at room temperature (as discussed in section 4.1.3.4).

#### 4.1.4.1.1 Determination of $K_{eq}$ at 20 °C

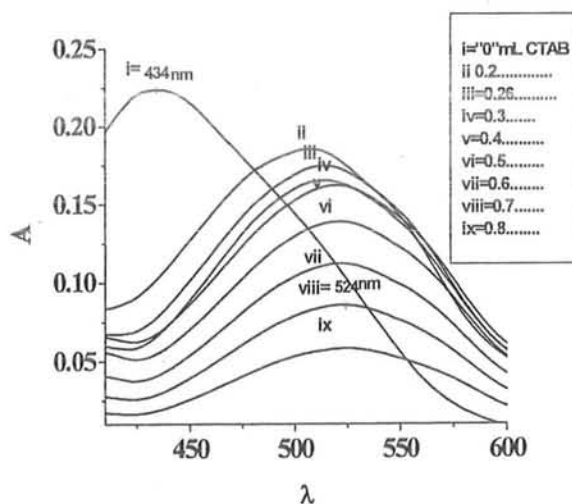


FIG.4.19. Plot of absorbance Vs. wavelength of different volume fractions of the complex made from nonequimolar mother solutions of ARS and CTAB ( $C_s^0 = 4 \times 10^{-4} \text{ mol.dm}^{-3}$ ,  $C_D^0 = 8 \times 10^{-5} \text{ mol.dm}^{-3}$ ) at 20°C.

FIG.4.19. shows the UV-spectra of a series of mixtures consisting of different amounts of both dye and surfactant at 20°C. The wavelength of maximum absorbance of the dye occurs at 434 nm as is shown in FIG.4.19. The wavelength of maximum absorbance changes from 434 nm (ARS) to about 524 nm for the complex. Calculations for  $\Delta A$  are shown in Table.4.10.

**Table 4.10. Calculations for the corrected absorbance of the complex formed as a result of interactions between ARS and CTAB ( $C_s = 4 \times 10^{-4}$  mol. dm<sup>-3</sup>,  $C_D = 8 \times 10^{-5}$  mol. dm<sup>-3</sup>) at 20°C**

$\Delta A = A_{\text{exp}} - \epsilon_D C_D^0 (1-X)$ $\epsilon_D C_D^0 = A_{\text{dye}} = 0.10322 \text{ at } 524 \text{ nm}$			
X	$A_{\text{exp}}$	$A_{\text{theor}}$	$\Delta A$
0	0	0	0
0.2	0.175	0.083	0.092
0.26	0.177	0.076	0.101
0.3	0.163	0.072	0.091
0.4	0.151	0.062	0.089
0.5	0.139	0.052	0.087
0.6	0.112	0.041	0.071
0.7	0.086	0.031	0.055
0.8	0.058	0.021	0.037
1	0	0	0

Table.4.10. shows calculations of the corrected absorbance ( $\Delta A$ ) for the complex at 524 nm at 20°C. A plot of " $\Delta A$ " Vs. "X" is shown in FIG.4.20.



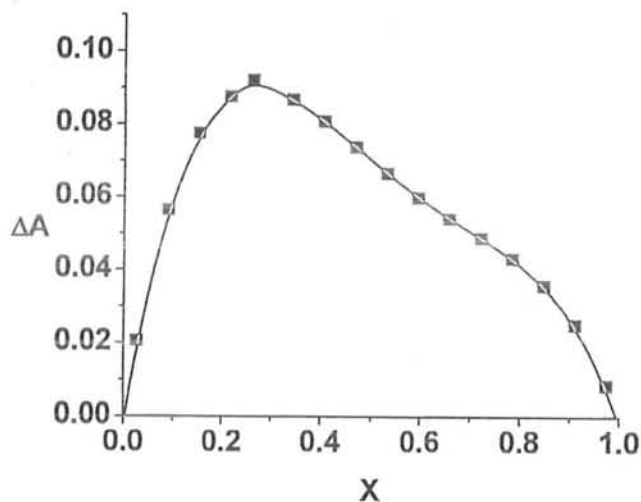


FIG.4.20. Job's plot ( $\Delta A$  Vs. volume fraction of surfactant solution) for nonequimolar mother solutions of ARS and CTAB in water at  $20^\circ\text{C}$ .  $C_S^\circ = 4 \times 10^{-4} \text{ mol.dm}^{-3}$ ,  $C_D^\circ = 8 \times 10^{-5} \text{ mol.dm}^{-3}$

From FIG.4.20. it is observed that using the nonequimolar mother solution of the dye and surfactant ( $C_S^\circ = 4 \times 10^{-4} \text{ mol.dm}^{-3}$ ,  $C_D^\circ = 8 \times 10^{-5} \text{ mol.dm}^{-3}$ ) the maximum absorbance occurs at 0.26 volume fraction of the surfactant solution at  $20^\circ\text{C}$ . So,  $X_m = 0.26$ . Now putting the value of " $X_m$ " in the corresponding equation for the determination of equilibrium complex formation constant equation (5),  $K_{eq}$  is calculated as

Table.4.11. Calculations of  $K_{eq}$  when  $C_S^\circ = 4 \times 10^{-4} \text{ mol.dm}^{-3}$  and  $C_D^\circ = 8 \times 10^{-5} \text{ mol.dm}^{-3}$  at  $20^\circ\text{C}$

T	$C_S^\circ / \text{mol. dm}^{-3}$	$C_D^\circ / \text{mol. dm}^{-3}$	$P = C_S^\circ / C_D^\circ$	$X_m$	$(p-1)(1-2X_m)$	$K_{eq} (\text{mol}^{-1}.\text{dm}^3)$
20	$4 \times 10^{-4}$	$8 \times 10^{-5}$	5.00	0.26	1.92	$1.50 \times 10^7$

From Table. 4.11. the value of equilibrium complex formation constant comes out to be  $1.50 \times 10^7 \text{ mol}^{-1}.\text{dm}^3$ .

#### 4.1.4.1.2

#### Determination of Equilibrium Complex formation constant at 25 °C

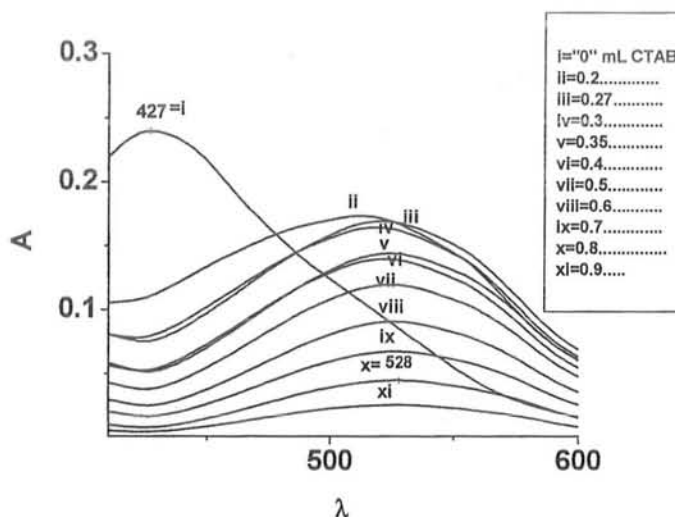


FIG.4.21. Plot of absorbance Vs. wavelength of different volume fractions of the complex made from nonequimolar mother solutions of ARS and CTAB ( $C_S^0=4 \times 10^{-4} \text{ mol.dm}^{-3}$ ,  $C_D^0=8 \times 10^{-5} \text{ mol.dm}^{-3}$ ) at 25°C

FIG.4.21. shows the UV-spectra of a series of mixtures consisting of different amounts of both dye and surfactant at 25°C. The wavelength of maximum absorbance of the dye occurs at 427 nm (curve i). The region from “ii” and “xi” shows the absorption spectra of the different fractions prepared by mixing the nonequimolar mother solutions of both dye and surfactant in various volume ratios. Complexation is observed at about 528 nm. Corrected absorbance ( $\Delta A$ ) is calculated for each mixture as shown in table.4.12.

Table 4.12. Calculations for the corrected absorbance of the complex formed as a result of interactions between ARS and CTAB ( $C_s^* = 4 \times 10^{-4} \text{ mol. dm}^{-3}$ ,  $C_D^* = 8 \times 10^{-5} \text{ mol. dm}^{-3}$ ) at 25°C

$\Delta A = A_{\text{exp}} - \epsilon_D C_D^0 (1-X)$ $\epsilon_D C_D^0 = A_{\text{dye}} = 0.08549 \text{ at } 528 \text{ nm}$			
X	$A_{\text{exp}}$	$A_{\text{theor}}$	$\Delta A$
0	0	0	0
0.2	0.167	0.068	0.099
0.27	0.170	0.062	0.108
0.3	0.162	0.060	0.102
0.35	0.152	0.055	0.097
0.4	0.139	0.051	0.088
0.5	0.119	0.043	0.076
0.6	0.091	0.034	0.057
0.7	0.068	0.026	0.042
0.8	0.045	0.017	0.028
0.9	0.026	0.009	0.017
1	0	0	0

Table.4.12. shows calculations of the corrected absorbance ( $\Delta A$ ) for the complex at 528 nm at 25°C.

A plot of “ $\Delta A$ ” Vs. “X” is shown in FIG.4.22.

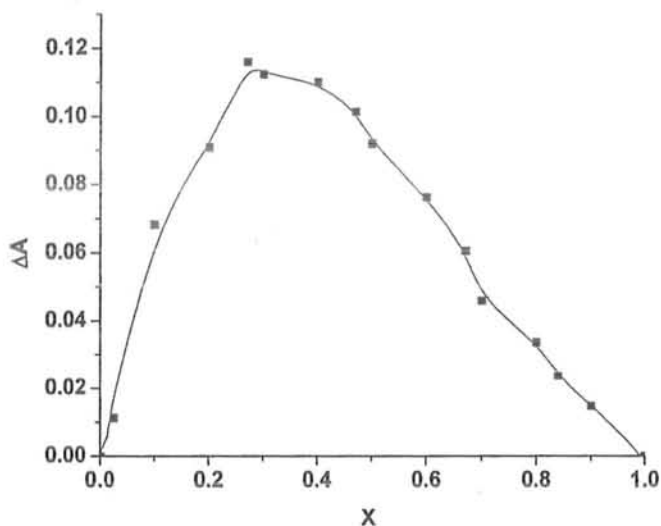


FIG.4.22. Job's plot ( $\Delta A$  vs. volume fraction of surfactant solution) for nonequimolar mother solutions of ARS and CTAB in water at  $25^{\circ}\text{C}$ .  $C_S^{\circ}=4\times10^{-4}\text{mol.dm}^{-3}$ ,  $C_D^{\circ}=8\times10^{-5}\text{mol.dm}^{-3}$

The maximum absorbance occurs at 0.27 volume fraction of the surfactant solution at  $25^{\circ}\text{C}$  as is shown in FIG.4.22. So,  $X_m = 0.27$ . Now putting the value of " $X_m$ " in equation (5) for the determination of equilibrium complex formation constant,  $K_{eq}$  is calculated as

Table.4.13. Calculations of  $K_{eq}$  when  $C_S^{\circ}=4\times10^{-4}\text{mol.dm}^{-3}$  and  $C_D^{\circ}=8\times10^{-5}\text{mol.dm}^{-3}$  at  $25^{\circ}\text{C}$

$T/^{\circ}\text{C}$	$C_S^{\circ}/\text{mol. dm}^{-3}$	$C_D^{\circ}/\text{mol. dm}^{-3}$	$P=C_S^{\circ}/C_D^{\circ}$	$X_m$	$(p-1)(1-2X_m)$	$K_{eq}(\text{mol}^{-1}.\text{dm}^3)$
25	$4\times10^{-4}$	$8\times10^{-5}$	5.00	0.27	1.84	$3.59 \times 10^6$

The value of equilibrium complex formation comes out to be  $3.59\times10^6\text{mol}^{-1}.\text{dm}^3$ .

4.1.4.1.3 Determination of Equilibrium Complex formation constant at 30 °C

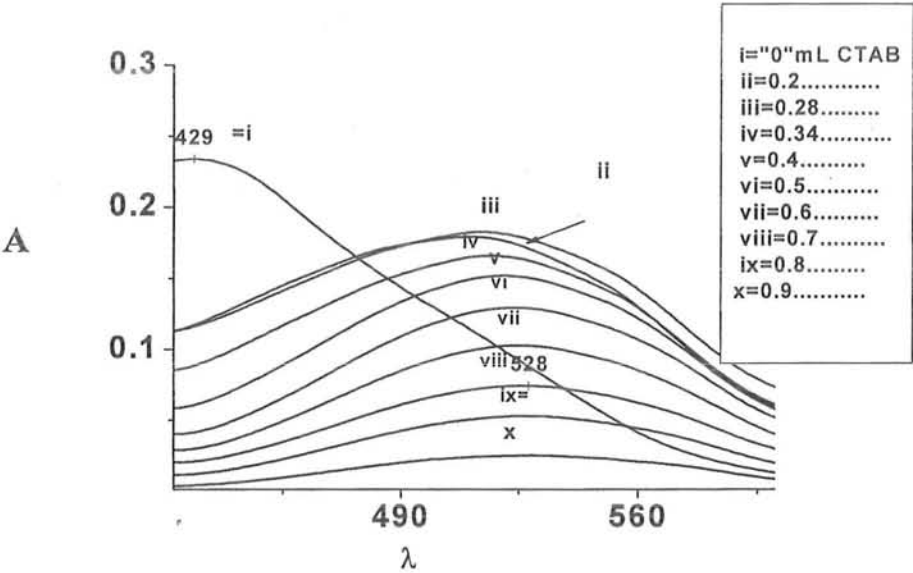


FIG.4.23. Absorption spectra of different volume fractions of the complex made from nonequimolar mother solutions of ARS and CTAB ( $C_S^{\circ}=4\times10^{-4}\text{ mol.dm}^{-3}$ ,  $C_D^{\circ}=8\times10^{-5}\text{ mol.dm}^{-3}$ ) at 30°C

UV-spectra of a series of mixtures consisting of different amounts of both dye and surfactant at 30°C is shown in FIG.4.23. The wavelength of maximum absorbance of the dye occurs at 429 nm (curve i) while a shift to about 528 nm (curves ii-x) is observed for the complex. Table.4.14. shows calculations for the exact absorbance or the corrected absorbance ( $\Delta A$ ).

Table 4.14. Calculations for the corrected absorbance of the complex formed as a result of interactions between ARS and CTAB ( $C_s^0 = 4 \times 10^{-4} \text{ mol. dm}^{-3}$ ,  $C_D^0 = 8 \times 10^{-5} \text{ mol. dm}^{-3}$ ) at  $30^\circ\text{C}$

$\Delta A = A_{\text{exp}} - \epsilon_D C_D^0 (1-X)$ $\epsilon_D C_D^0 = A_{\text{dye}} = 0.087729 \text{ at } 528 \text{ nm}$			
X	$A_{\text{exp}}$	$A_{\text{theor}}$	$\Delta A$
0	0	0	0
0.2	0.169	0.070	0.099
0.28	0.171	0.063	0.108
0.34	0.162	0.058	0.104
0.4	0.150	0.053	0.097
0.5	0.129	0.044	0.085
0.6	0.103	0.035	0.068
0.7	0.074	0.026	0.048
0.8	0.053	0.017	0.036
0.9	0.025	0.009	0.016
1	0	0	0

Table.4.14. shows calculations of the corrected absorbance ( $\Delta A$ ) for the complex at 528 nm at  $30^\circ\text{C}$ . A plot of " $\Delta A$ " Vs. " $X$ " is shown in FIG.4.24.

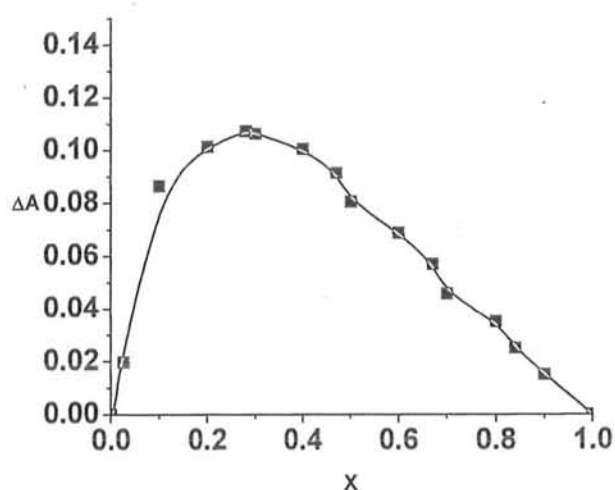


FIG.4.24. Job's plot ( $\Delta A$  Vs.  $X$ ) in water at  $30^\circ\text{C}$ .  $C_s^0 = 4 \times 10^{-4} \text{ mol. dm}^{-3}$ ,  $C_D^0 = 8 \times 10^{-5} \text{ mol. dm}^{-3}$

From FIG.4.24. it is observed that at 30°C the maximum absorbance occurs at 0.28 volume fraction of the surfactant solution. So,  $X_m = 0.28$ . Putting the value of “ $X_m$ ” in the equation (5) for the determination of equilibrium complex formation constant,  $K_{eq}$  is calculated s

Table.4.15. Calculations of  $K_{eq}$  when  $C_s^{\circ}=4\times10^{-4}\text{mol.dm}^{-3}$  and  $C_D^{\circ}=8\times10^{-5}\text{mol.dm}^{-3}$  at 30°C

$T/^{\circ}\text{C}$	$C_s^{\circ}/\text{mol. dm}^{-3}$	$C_D^{\circ}/\text{mol. dm}^{-3}$	$P= C_s^{\circ}/ C_D^{\circ}$	$X_m$	$(p-1)(1-2X_m)$	$K_{eq}(\text{mol}^{-1}.\text{dm}^3)$
30	$4\times10^{-4}$	$8\times10^{-5}$	5.00	0.28	1.76	$1.53 \times 10^6$

Equilibrium complex formation constant  $K_{eq}$  comes out to be  $1.53\times10^6\text{mol}^{-1}.\text{dm}^3$ .

4.1.4.1.4 Determination of Equilibrium Complex formation constant at 35 °C

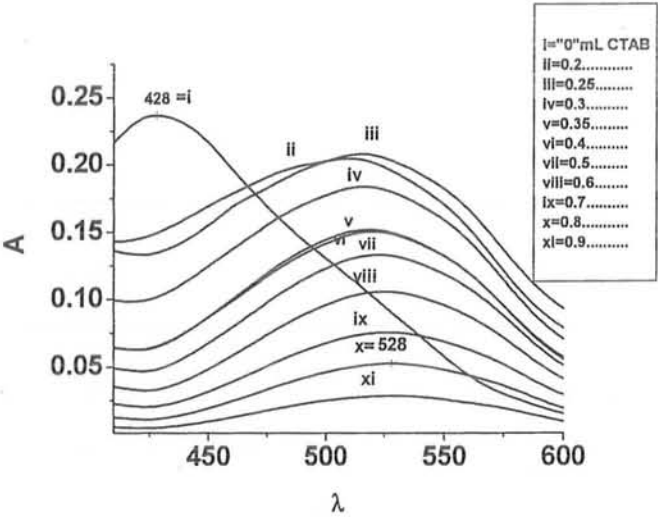


FIG.4.25. Absorption spectra of different volume fractions of the complex made from nonequimolar mother solutions of ARS and CTAB ( $C_s^{\circ}=4\times10^{-4}\text{mol.dm}^{-3}$ ,  $C_D^{\circ}=8\times10^{-5}\text{mol.dm}^{-3}$ ) at 35°C

FIG.4.25. shows the UV-spectra of a series of mixtures consisting of different amounts of both dye and surfactant at 35°C. Curve "i" is the absorption spectra of the dye. The wavelength of maximum absorbance of the dye occurs at 428 nm. The region from "ii" and "xi" shows the absorption spectra of the different fractions prepared by mixing the nonequimolar mother solutions of both dye and surfactant in various volume ratios. The wavelength of maximum absorbance changes from 428 nm for the dye alone to about 528nm for the complex. Table.4.16. shows calculations for the exact absorbance or the corrected absorbance ( $\Delta A$ ).

**Table 4.16. Calculations for the corrected absorbance of the complex formed as a result of interactions between ARS and CTAB ( $C_s^* = 4 \times 10^{-4}$  mol. dm<sup>-3</sup>,  $C_D^* = 8 \times 10^{-5}$  mol. dm<sup>-3</sup>) at 35°C**

$\Delta A = A_{\text{exp}} - \epsilon_D C_D^0 (1-X)$ $\epsilon_D C_D^0 = A_{\text{dye}} = 0.090199 \text{ at } 528 \text{ nm}$			
X	A <sub>exp</sub>	A <sub>theor</sub>	ΔA
0	0	0	0
0.2	0.142	0.072	0.070
0.25	0.154	0.068	0.086
0.3	0.167	0.063	0.104
0.35	0.180	0.059	0.121
0.4	0.149	0.054	0.095
0.5	0.132	0.045	0.087
0.6	0.106	0.036	0.070
0.7	0.076	0.027	0.049
0.8	0.053	0.018	0.035
0.9	0.029	0.009	0.020
1	0	0	0



Table.4.16. shows calculations of the corrected absorbance ( $\Delta A$ ) for the complex at 528 nm at 35°C. A plot of " $\Delta A$ " Vs. " $X$ " is shown in FIG.4.26.

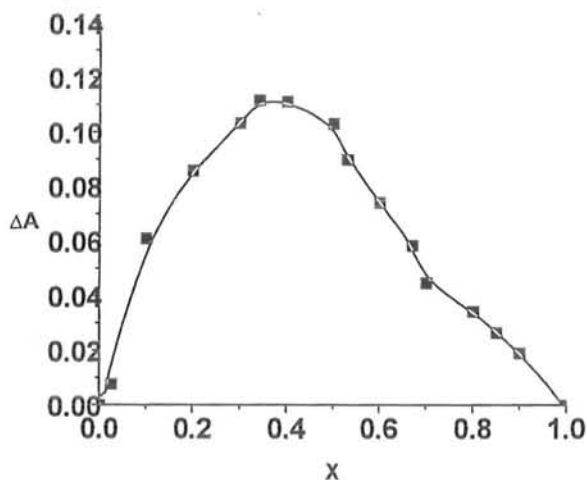


FIG.4.26. Job's plot ( $\Delta A$  vs. volume fraction of surfactant solution) for nonequimolar mother solutions of ARS and CTAB in water at 35°C.  $C_S^0=4 \times 10^{-4} \text{ mol.dm}^{-3}$ ,  $C_D^0=8 \times 10^{-5} \text{ mol.dm}^{-3}$

From FIG. 4.26. it is observed that the maximum absorbance occurs at 0.34 volume fraction of the surfactant solution at 35°C. So,  $X_m = 0.34$ . Now putting the value of " $X_m$ " in equation for the determination of equilibrium complex formation constant (equation 5),  $K_{eq}$  is calculated as

Table.4.17. Calculations of  $K_{eq}$  when  $C_S^0=4 \times 10^{-4} \text{ mol.dm}^{-3}$  and  $C_D^0=8 \times 10^{-5} \text{ mol.dm}^{-3}$  at 35°C

$T/^{\circ}\text{C}$	$C_S^0 / \text{mol. dm}^{-3}$	$C_D^0 / \text{mol. dm}^{-3}$	$P= C_S^0 / C_D^0$	$X_m$	$(p-1)(1-2X_m)$	$K_{eq}(\text{mol}^{-1}.\text{dm}^3)$
35	$4 \times 10^{-4}$	$8 \times 10^{-5}$	5.00	0.34	1.26	$1.17 \times 10^5$

The complex formation constant comes out to be  $1.17 \times 10^5 \text{ mol}^{-1}.\text{dm}^3$  at  $35^\circ\text{C}$ .

4.1.4.1.5      **Determination of Equilibrium Complex formation constant at  $40^\circ\text{C}$**

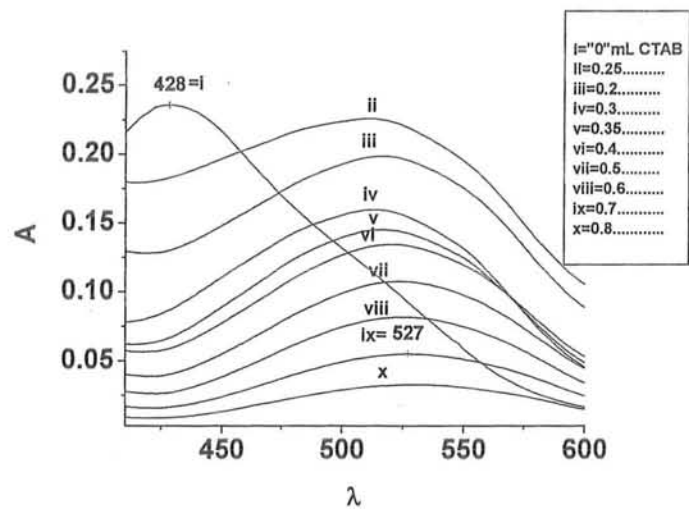


FIG.4.27. Plot of absorbance VS wavelength of the different volume fractions of the complex made from nonequimolar mother solutions of ARS and CTAB ( $C_s^\circ=4\times10^{-4}\text{mol}.\text{dm}^{-3}$ ,  $C_D^\circ=8\times10^{-5}\text{mol}.\text{dm}^{-3}$ ) at  $40^\circ\text{C}$

FIG.4.27. shows the UV-Visible spectra of a series of mixtures consisting of different amounts of both dye and surfactant at  $40^\circ\text{C}$ . Curve ‘i’ shows the absorption spectra of pure dye. The wavelength of maximum absorbance of the dye occurs at 428 nm. The region from “ii” and “x” shows the absorption spectra of the different fractions prepared by mixing the nonequimolar mother solutions of both dye and surfactant in various volume ratios. The wavelength of maximum absorbance changes from 428 nm for the dye alone to about 527 nm for the complex. Table.4.18. shows calculations for the exact absorbance or the corrected absorbance ( $\Delta A$ ).

Table. 4.18. Calculations for the corrected absorbance of the complex formed as a result of interactions between ARS and CTAB ( $C_s = 4 \times 10^{-4} \text{ mol. dm}^{-3}$ ,  $C_D = 8 \times 10^{-5} \text{ mol. dm}^{-3}$ ) at  $40^\circ\text{C}$

$\Delta A = A_{\text{exp}} - \epsilon_D C_D^0 (1-X)$ $\epsilon_D C_D^0 = A_{\text{dye}} = 0.091119 \text{ at } 528 \text{ nm}$			
X	$A_{\text{exp}}$	$A_{\text{theor}}$	$\Delta A$
0	0	0	0
0.2	0.174	0.073	0.101
0.25	0.179	0.068	0.111
0.3	0.182	0.064	0.118
0.36	0.187	0.058	0.129
0.4	0.150	0.055	0.095
0.5	0.133	0.045	0.088
0.6	0.107	0.036	0.071
0.7	0.082	0.027	0.055
0.8	0.055	0.018	0.037
1	0	0	0

Table.4.18. shows calculations of the corrected absorbance ( $\Delta A$ ) for the complex at 528 nm at  $40^\circ\text{C}$ . A plot of " $\Delta A$ " Vs. " $X$ " is shown in FIG.4.28.

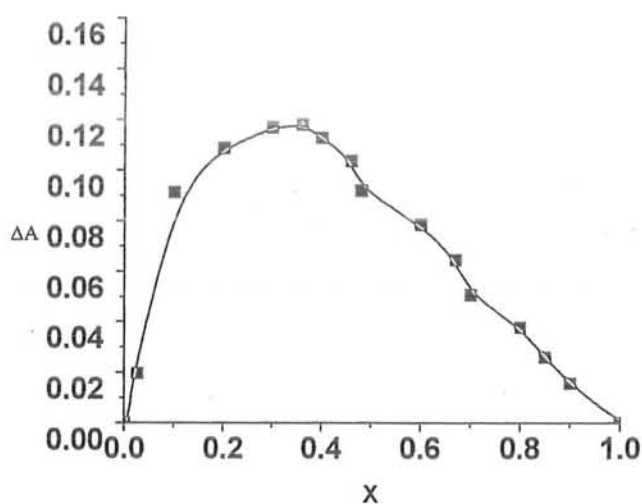


FIG.4.28. Job's plot ( $\Delta A$  Vs. volume fraction of surfactant solution) for nonequimolar mother solutions of ARS and CTAB in water at  $40^{\circ}\text{C}$ .  $C_S^{\circ}=4\times 10^{-4}\text{mol.dm}^{-3}$ ,  $C_D^{\circ}=8\times 10^{-5}\text{mol.dm}^{-3}$

From FIG. 4.28. it is observed that the maximum absorbance is shown by the complex at 0.36 volume fraction of the surfactant solution at  $40^{\circ}\text{C}$ . So,  $X_m = 0.36$ . Now putting the value of " $X_m$ " equation (5)

Table.4.19. Calculations of  $K_{eq}$  when  $C_S^{\circ}=4\times 10^{-4}\text{mol.dm}^{-3}$  and  $C_D^{\circ}=8\times 10^{-5}\text{mol.dm}^{-3}$  at  $40^{\circ}\text{C}$

$T/^{\circ}\text{C}$	$C_S^{\circ}/\text{mol. dm}^{-3}$	$C_D^{\circ}/\text{mol. dm}^{-3}$	$P= C_S^{\circ}/ C_D^{\circ}$	$X_m$	$(p-1)(1-2X_m)$	$K_{eq}(\text{mol}^{-1}.\text{dm}^3)$
40	$4\times 10^{-4}$	$8\times 10^{-5}$	5.00	0.36	1.12	$7.23\times 10^4$

The equilibrium complex formation comes out to be  $7.23\times 10^4\text{mol}^{-1}.\text{dm}^3$  at  $40^{\circ}\text{C}$ .

The  $K_{eq}$  at all the mentioned different temperatures are given in table.4.20 for convenience

**Table.4.20. Values of  $K_{eq}$  at different temperatures**

Temperature /°C	$K_{eq}$ (mol-1.dm3)
20	$1.50 \times 10^7$
25	$3.59 \times 10^6$
30	$1.53 \times 10^6$
35	$1.17 \times 10^5$
40	$7.23 \times 10^4$

Table.4.20. shows the combined representation of the equilibrium complex formation constant ( $K_{eq}$ ) obtained so far at different temperatures using Job's Method. The table shows that the complexation constant decreases with increasing temperature. Since we have supposed that the major contribution is by electrostatic forces in the complexation process in the premicellar region between the cationic surfactant (CTAB) and anionic dye (ARS) , the results we have obtained are in accordance with most published work that electrostatic interactions gets weakened with increasing temperature [1,12,28].

#### **4.1.4.2 Thermodynamic Parameters**

On the basis of  $K_{eq}$  calculated at different temperatures, various thermodynamic parameters ( $\Delta G$ ,  $\Delta H$ , and  $\Delta S$ ) are calculated. These thermodynamic parameters are helpful in suggesting the possible mechanism of interactions between ARS and CTAB.

Gibbs free energy ( $\Delta G$ ) is calculated using the following equation.

$$\Delta G = -RT \ln K_{eq}$$

Where “R” is general gas constant, “T” is temperature in Kelvin and “K<sub>eq</sub>” is the equilibrium complex formation constant.

Enthalpy “Δ H” is calculated using Van’t Hoff equation , which is given as

$$\ln K_{eq} = \frac{-\Delta H}{RT}$$

A plot is made between lnK<sub>eq</sub> and 1/T. Multiplying slope with general gas constant gives the value of “Δ H”.

Entropy of the system “ΔS” is calculated

$$\Delta S = \frac{\Delta H - \Delta G}{T}$$

FIG.4.29. shows plot of lnK<sub>eq</sub> Vs. 1/T for the determination of “Δ H”.

**Calculation of “ΔH” using Van’t Hoff Plot**

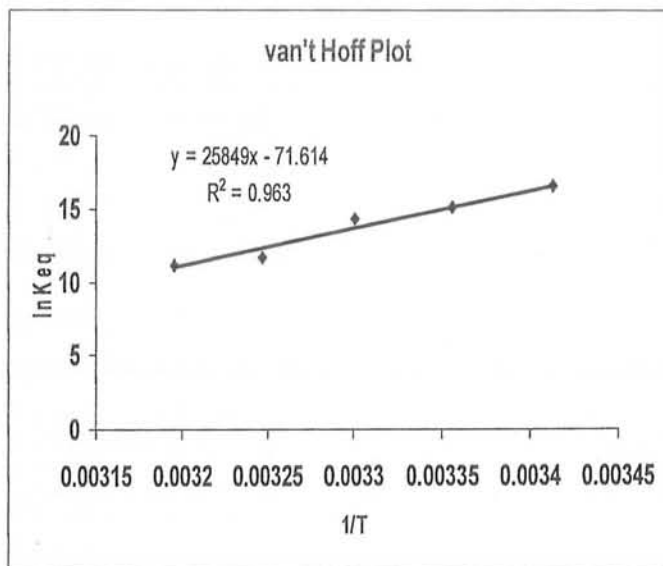


**FIG.4.29. Van’t Hoff Plot for the electrostatic complex between ARS and CTAB in aqueous medium**

All the thermodynamic parameters are given combinely in Table. 4.21.

**Table.4.21. Calculations of different thermodynamic parameters**

Temperature/K	$K_{eq}$ ( $\text{mol}^{-1}.\text{dm}^3$ )	$-\Delta G$ ( $\text{kJ mol}^{-1}$ )	$-\Delta H$ ( $\text{kJ mol}^{-1}$ )	$-\Delta S$ ( $\text{kJmol}^{-1}\text{K}^{-1}$ )
293	$1.50 \times 10^7$	40	215	0.59726
298	$3.59 \times 10^6$	37	-	0.59731
303	$1.53 \times 10^6$	36	-	0.59076
308	$1.17 \times 10^5$	30	-	0.60065
313	$7.23 \times 10^4$	29	-	0.59425

From Table.4.21 it can be seen that the negative value of  $\Delta G$  decreases with increasing temperature. It suggests that the reaction is highly spontaneous at the low temperature. Negative value of  $\Delta H$  indicates that the reaction is exothermic which is also cleared from the  $k_{eq}$  value calculated at different temperatures i.e., as temperature increases the equilibrium composition constant decreases. The negative  $\Delta S$  suggests that hydrophobic interactions do not play a major role in the interaction between dye and surfactant [30]. These points are in the favor of our suggested mechanism that electrostatic interactions play major role in the complexation of oppositely charged dye (ARS) and surfactant (CTAB) .The negative  $\Delta S$  also indicates that the system is highly stable .On the basis of these thermodynamic parameters discussed so far and the FTIR spectra of ARS,CTAB and ARS-CTAB complex we have proposed a possible mechanism for the interactions between Alizarin Red S and Cetyltrimethylammonium bromide in aqueous medium, which is given in FIG. 4.33.

## Section II

### 4.2 Infrared Spectroscopy

The intensity of IR band is a measure of the probability of transition to the next vibrational level, and is proportional to the square of the change in dipole moment of the molecule during vibration. If there is no change of dipole moment during vibration, then the electromagnetic radiation cannot interact with the vibration, and thus there is no absorption, i.e., the vibration is infrared-inactive or forbidden. For example, the absorption stretching of the carbon triple bond carbon does not appear in the spectra of symmetrically substituted dialkylacetylenes. Bonds involving only small changes of dipole moment during vibration, absorbs weakly. Absorption bands caused by stretching vibrations of polar groups are usually the most intense bands in the IR spectrum, but the intensities of even the most polar groups are two to three factors of ten weaker than those of the most intense electronic transitions (UV-VIS spectroscopy).

An IR spectrum may be divided into two parts.

#### (i) The functional group region

The part ranging from  $1600\text{--}4000\text{ cm}^{-1}$  is known as the functional group region.

#### (ii) The Fingerprint region

The region ranging from  $625\text{--}1600\text{ cm}^{-1}$  is known as the fingerprint region.

The initial approach is usually to examine the functional group region because in this region, most compounds have only a few strong bands due to the characteristic stretching vibrations of their functional groups. These bands can be readily assigned because the various functional groups absorb at specific positions in the functional group region of



the spectrum. For example the absorptions due to carbonyl functional group occurs in the region  $1600\text{-}1900\text{ cm}^{-1}$ .

The fingerprint region is called so because it provides a set of absorption bands that is uniquely characteristic of each compound, and serves as its fingerprint. Although similar compounds may show very similar spectrum in the functional group region, there will almost always be a noticeable difference in the fingerprint region.

IR spectroscopy does not provide an absolute method for elucidating the exact structure of the compound. The information derived from it, though often correct, is always tentative, and is used together with evidences obtained by physical, chemical, or other spectroscopic means. Perhaps the most powerful function of the IR spectroscopy is to establish exclusively the identity of two samples which have identical spectra when determined under identical conditions, since complete superimposability of two spectra, particularly in the fingerprint region, provides confirmation of identity. Structural information is mainly derived from the presence or absence of characteristic absorption bands of various functional groups. A knowledge of the band position of common functional groups together with that of modifying factors will be invaluable.

#### **4.2.1 Applications of Infrared Spectroscopy**

The numerous applications of IR spectroscopy include:

##### **(i) Structure determination**

IR spectroscopy is mainly used for the determination of structures of organic compounds by correlation and interpretation of spectra.

**(ii) Identification of compounds**

The identity of a compound can often be established by the comparison of its infrared spectrum with that of an authentic sample.

**(iii) Detection of impurities**

The presence of absorption bands at positions where the compound is not expected to absorb indicates the presence of impurities. The difference method can be used to reveal the actual spectrum of the impurity. When the impure substance is placed in the sample beam and the same thickness of pure sample placed in the reference beam, the spectrum of impurity is recorded.

**(iv) Progress of a reaction**

The progress of most reactions can be followed readily by examining the IR spectra of aliquots withdrawn from the reaction mixture.

**(v) Percentage composition of a mixture**

If Beer's law is obeyed, the spectrum of a mixture is that resulting from the superimposition of the spectra of pure components. A characteristic band is chosen for each component and its intensity measured in the pure state or in mixture in mixtures of known composition [41].

#### **4.2.1.1 FTIR Study OF ARS-CTAB Complex**

Since UV-Vis spectroscopic study revealed the complex formation between ARS and CTAB in premicellar region in aqueous medium as discussed in part II of our experimental portion, our next approach was to apply FTIR spectroscopic technique to see whether this technique give any clue in the formation of the complex between ARS and CTAB or not. The FTIR spectra of ARS and CTAB were taken in the solid form by

mixing them with one fourth portion of KBR, while that of the complex was taken by placing a drop of the mixture of the complex on KBR pellet. These spectra are shown as:

#### 4.2.1.1.1 FTIR spectrum of CTAB

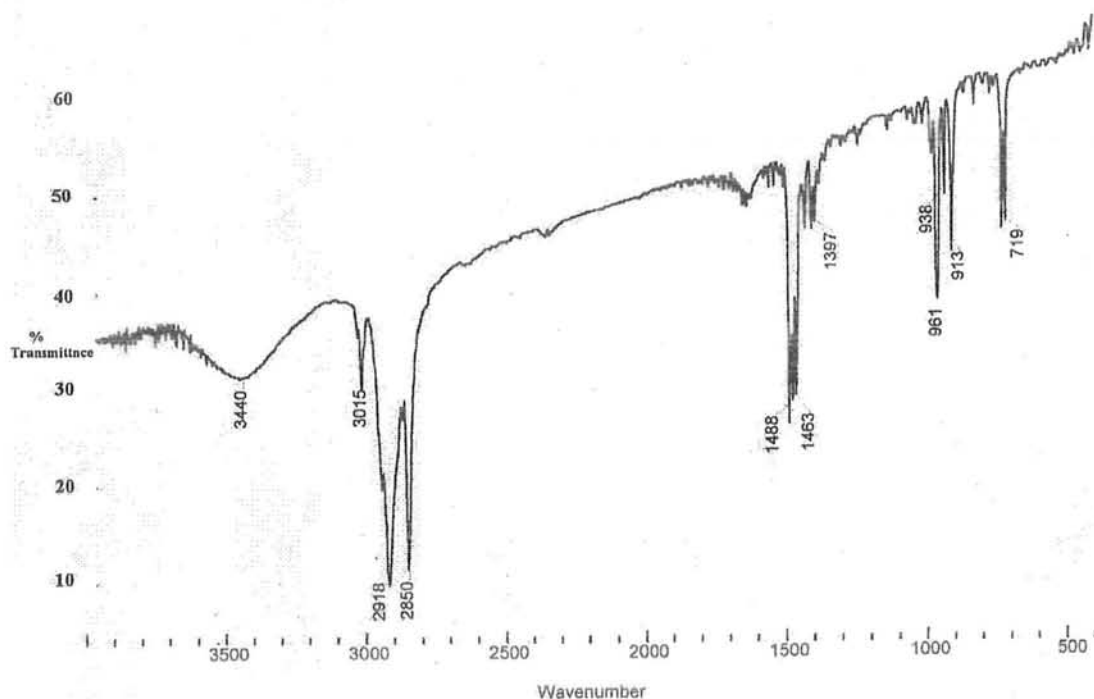


**FIG. 4.30. FTIR Spectrum of CTAB**

The FTIR spectrum of CTAB shows characteristic bands in the region 2850-3500 due to C-H stretching vibrations, including both symmetric and asymmetric stretching. The high frequency band is due to asymmetric str, while the other is due to symmetric C-H str. The asymmetric C-H stretch due to CH<sub>3</sub> group occurs near 2962 cm<sup>-1</sup>, while that due to CH<sub>2</sub> group occurs near 2926 cm<sup>-1</sup>. In the FTIR spectrum of CTAB (FIG.4.30) the intensity of the band due to asymmetric CH<sub>2</sub> is higher (2918 cm<sup>-1</sup>) which is an indication of the presence of CH<sub>2</sub> group in excess compared to CH<sub>3</sub> group. The symmetric stretching vibrations due to CH<sub>3</sub> and CH<sub>2</sub> occur, respectively, near 2872 and 2853 cm<sup>-1</sup>. In the above spectrum (FIG.4.30) for CTAB the band near 2853 cm<sup>-1</sup>, i.e., 2851 cm<sup>-1</sup> is intense,

#### 4.2.1.1.2 FTIR spectrum of ARS

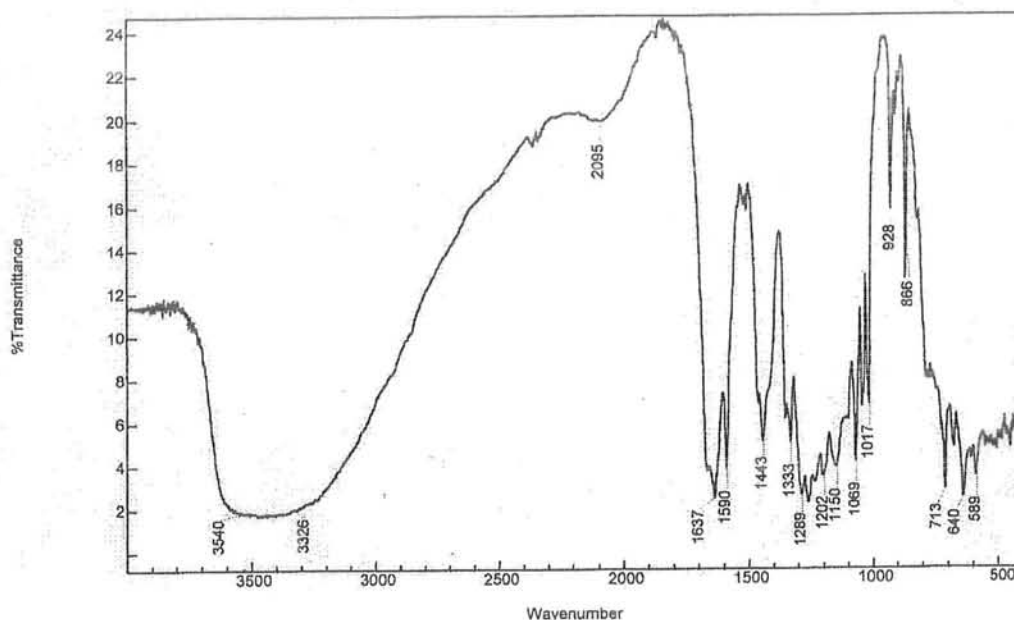


FIG. 4.31. FTIR Spectrum of ARS

FIG.4.31. shows FTIR spectrum of ARS. FTIR spectrum of ARS shows characteristic bands at 3326-3540  $\text{cm}^{-1}$  due to bonded OH group stretching. The band at about 1637  $\text{cm}^{-1}$  indicates the presence of carbonyl functional group, and the observed in the region 1443-1590  $\text{cm}^{-1}$  is due to the in-plane skeletal vibrations of the aromatic ring. These vibrations involve expansion and contraction of the C-C bonds within the ring. The most prominent and informative bands in the spectra of aromatic compounds occur in the 700-900  $\text{cm}^{-1}$  region due to the out-of-plane bending of the ring C-H bonds. These bands are also observed in the above FTIR spectrum of ARS. Since in the molecular structure of ARS p-benzoquinone is present, so the characteristic band due to this group is observed

at  $866\text{ cm}^{-1}$ . The band observed at  $1333\text{ cm}^{-1}$  is assigned to sulphone asymmetric stretching.

#### 4.2.1.1.3 FTIR spectrum of ARS-CTAB complex

Bio-Rad Merlin

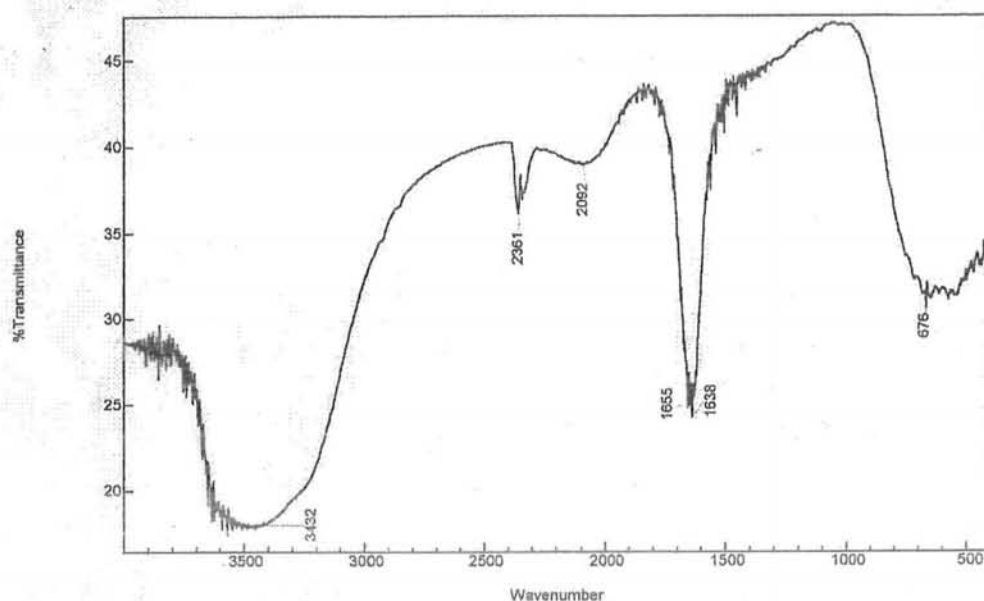


FIG. 4.32. FTIR spectrum of ARS-CTAB complex in aqueous medium

FIG.4.32 shows FTIR spectrum of ARS-CTAB complex. FTIR spectra of the complex was taken in solution form, so due to presence of moisture some fine structures observed in the FTIR spectra of ARS and CTAB individually are missing but the appearance of ridges like structures indicate their presence, like Ridge at  $2850\text{--}2918\text{ cm}^{-1}$  indicate C-H stretching, the region  $1300\text{--}1463\text{ cm}^{-1}$  shows C-H bending and the region above  $1600\text{ cm}^{-1}$  indicates the presence of carbonyl functional group. If we correlate the FTIR spectra of the ARS and CTAB taken alone with that of the complex one can find easily

spectra of the ARS and CTAB taken alone with that of the complex one can find easily that the presence of the carbonyl functional group at its characteristic position indicates that this group has not taken part in the complex formation between the ARS and CTAB. Otherwise a change would have been observed if this group or other group in its vicinity in the molecular structure of ARS was involved in the complexation process. The missing of fine structures in the spectrum of the complex in the fingerprint region is probably due to the presence of the complex in the solution form.

#### 4.3 Suggestion for the possible mechanism of interactions between ARS and CTAB

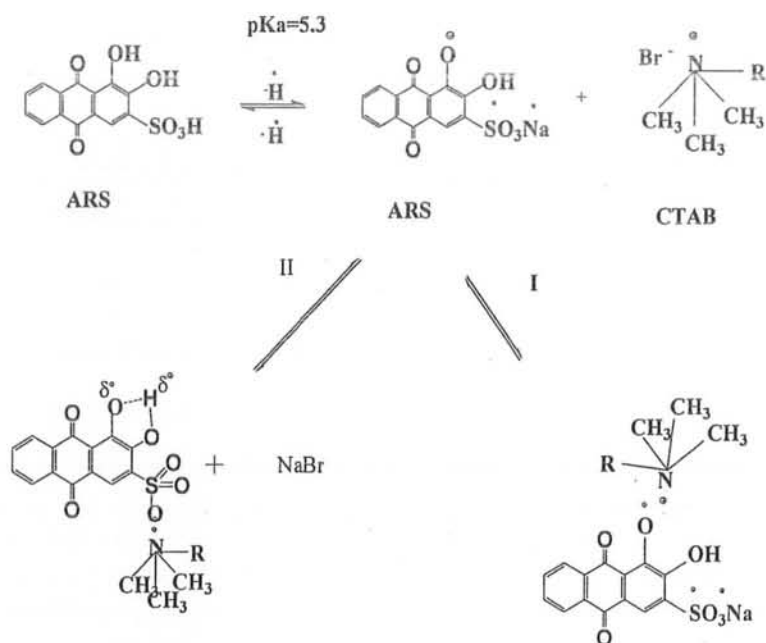


FIG.4.33. Possible mechanism of the interaction between ARS and CTAB

On the basis of FTIR spectra as mentioned above a mechanism is proposed which helps in explaining the interaction between ARS and CTAB in the premicellar region.

FIG.4.33 is the diagrammatic representation of this proposed mechanism. Two  $pK_a$  values are reported for ARS. One  $pK_a$  is 5.3 and the other is 10. In aqueous medium ARS is in monoionic form. In the mentioned mechanism (FIG.4.33) two pathways are shown via which cationic surfactant CTAB can interact with ARS. Pathway "I" suggests that CTAB can make interaction with the negatively charged oxygen rather than with sulphonate group. But since in the vicinity of this negatively charged oxygen a hydroxyl group is present, so most probably intra hydrogen bonding is expected. Even if we don't think of intra hydrogen bonding, the other possibility is that since we are conducting our experiment in aqueous medium, the water molecules are surrounding this negatively charged oxygen. So it is not free. Then the only site which is left is the sulphonate group, at which CTAB can make electrostatic interaction with ARS. So pathway II is preferred compared to pathway I.

The information of our interest is that the band which appears due to carbonyl functional group in the individual spectrum of Alizarin Red S (ARS) is still present at its own position in the FTIR spectrum of the complex, although other fine structures are missing in the spectrum of the complex. Since carbonyl functional group exists at their own position, it means that no big change has occurred in its vicinity. If CTAB was to attack the negatively charged oxygen, which is in the vicinity of Carbonyl functional group, then of course one would have observed a change in the band due to carbonyl functional group. Since this change is not observed in the spectrum of the complex so we can say that most probably the electrostatic interaction is between the positively charged ammonium of the CTAB and the negatively charged sulphonate group of the dye (ARS).

#### 4.4 Conclusions

It has been shown that the interaction between Alizarin Red S and Cetyltrimethylammonium bromide in the premicellar region results in 1:1 ion-pair association. The changing concentrations using equimolar mother solutions of both dye and surfactant have no effect on the composition of the complex; i.e., in all cases 1:1 complex is formed. Both hydrophobic and electrostatic interactions are involved but in case of oppositely charged dye and surfactant the major contribution is of electrostatic origin as is also evident from the negative value of entropy. An increase in temperature reduces the tendency to ion-pair formation. UV-VIS spectroscopy indicated the occurrence of complexation between ARS and CTAB as indicated by a significant shift of about 100 nm in the wavelength of maximum absorbance of the dye. Job's method which is an important application of UV-VIS spectroscopy helped in the determination of composition of the complex plus its equilibrium complex formation constant. And the FTIR analysis of the complex helped us in suggesting the possible mechanism of interactions between ARS and CTAB and finally proposing the structure of the complex in aqueous medium. The correlation of UV-VIS spectroscopy and IR spectroscopy reveals that the combine use of the two techniques is helpful in determining the possible structure and the pathway leading to these complex structures. On the basis of the proposed mechanism and suggested structure of the complex it can be concluded that the importance of electrical forces is basically to bring the dye anion and the surfactant cation close enough (in the premicellar region) to enable the action of short range interactions (hydrophobic interactions), which act mainly in the micellar region.



- [35] Moater, E.I.; Olteanu, M., Ionita, I., Radulescu, C., *Rev. Chim*, **2005**, *56*, 1054-1057.
- [36] Kartal, C.; Akbas, H., *Dyes Pigments*, **2005**, *65*, 191-195.
- [37] Gokturk, S., *J. Photochem. Photobiol. A-Chem.* **2005**, *169*, 115-121.
- [38] Yang, J.; *J. Colloid Interface Sci.* **2004**, *274*, 237-243.
- [39] Oakes, J.; Gratton, P., Dixon, S., *Color. Technol*, **2003**, *119*, 301-306.
- [40] Younas, M.; *Organic Spectroscopy*; AHP International (Pvt) Limited: Al-Fazal Market, Urdu Bazar, Lahore, **1998**; p 63-102.